Supplementary Information for

Runx3 is required for oncogenic Myc upregulation in *p53*-deficient osteosarcoma

Shohei Otani[†], Yuki Date[†], Tomoya Ueno, Tomoko Ito, Shuhei Kajikawa, Keisuke Omori, Ichiro Taniuchi, Masahiro Umeda, Toshihisa Komori, Junya Toguchida, Kosei Ito*

[†]These authors contributed equally.

*Correspondence to: itok@nagasaki-u.ac.jp

Department of Molecular Bone Biology, Graduate School of Biomedical Sciences, Nagasaki University, 1-7-1 Sakamoto, Nagasaki, 852-8588, Japan.

This file includes:

Supplementary Materials & Methods

Supplementary Figures 1-13

Supplementary Tables 1-4

Materials and methods

Mouse lines

A *Runx3(P1)*-deleted mouse line was generated that systemically lacked the 3' region of the *Runx3(P1)* exon 1, which encodes the N-terminal region of Runx3(P1) (MASNSIFDSFPNYTPTFIR). The targeting vector harboring exon 1 and a *Loxp/FRT*-flanked Neomycin resistance gene (*Neo*) was electroporated into Bruce-4 ES cells (C57BL/6). Digested genomic DNA of targeted ES cells was subjected to Southern blotting using 5' or 3' alkaline phosphatase-labeled probes (386 bp or 536 bp), which were generated by PCR using primers 5'-TGTAATGCTCTGTCCTTTATCTGTG -3' and 5'-CTGACTGTCTTCTGGTTAGAACGAT-3', or 5'-GATGTAGCACCCAGTATCTCAAAGC-3' and 5'-CAGATGCTAGACTTCCTTCTCAGTTA-3', respectively, and mouse genome DNA as the template. To remove the *Loxp*-flanked *Neo*, the offspring (F1) was crossed with *CAG*-Cre transgenic mice. The *Runx3(P1)*$^{\Delta}$ and wild-type alleles of *Runx3(P1)*$^{\Delta/+}$ mice were detected by PCR using primers 5'-CTCAAACAGACAAAGGTCAGATGTA-3' and 5'-ATGTTGAGCAGATTCTCATAGAGG-3', yielding products of 205 bp and 642 bp, respectively.

An mR1-mutated mouse line was generated by homologous recombination. The targeting vector harboring a *BglII*-replaced mR1 and an *FRT*-flanked neomycin resistance gene (*Neo*) were electroporated into Bruce-4 ES cells. Digested genomic DNA of targeted ES cells was subjected to Southern blotting using 5' or 3' alkaline phosphatase-labeled probes (483 bp or 380 bp), which were generated by PCR using primers 5'-TTTGACATAGCTAGTGAGACAGCAG -3' and 5'-CAGGAGGAGATATTTGAGGTTGTTA-3', or 5'-CAGGATGCTTTCTGTGGATAGTAAT-3' and 5'-CTCTGAACCTTTGTATGTCCTTGTT-3', respectively, and mouse genome DNA as the template. To remove the *FRT*-flanked *Neo*, F1 was crossed with *CAG*-FLP transgenic mice. The mutant and wild-type alleles of *mR1*$^{m/+}$ mice were detected by PCR using primers 5'-GGTTTAGAGTGTAGAAGGGAGGTGT-3' and 5'-ATTGCTGACTTGGAGGAGAGAG-3', yielding products of 188 bp and 110 bp, respectively.

Genome-edited mR1-, mR2-, or mR3-mutant mouse line was generated by intra-cytoplasmic injection of fertilized zygotes with Alt-R S.p. HiFi Cas9 Nuclease (Integrated DNA

Technologies), an annealed pair of Alt-R CRISPR-Cas9 tracrRNA and Alt-R CRISPR-Cas9 crRNA (Integrated DNA Technologies), and ssDNA flanking the target site. DNA target sequences upstream of each PAM site (20 bases) and the corresponding ssDNA sequences are shown below.

mR1

crRNA: 5'-CTGCGTATATCAGTCACCGC-3'

ssDNA (150-mer):

5'-GGCCGCCCGGGACGTGCGTGACGCGGTCCAGGGTACATGGCGTATTGTGT
GGAGCGAGGCAGCTGTTCCACCagatctGACTGATATACGCAGGGCAAGAACACAGTTC
AGCCGAGCGCTGCGCCCGAACAACCGTACAGAAAGGGAAAG-3'

mR2

crRNA: 5'-AGGGTGATCAACCGCAGATG-3'

ssDNA (150-mer):

5'-TATACGTGGCAGTGAGTTGCTGAGCAATTTTAATAAAATTCCAGACATCGT
TTTTCCTGCATAGACCTCATCagatctTGATCACCCTCTATCACTCCACACACTGAGCGG
GGGCTCCTAGATAACTCATTCGTTCGTCCTTCCCCCTTT-3'

mR3

crRNA: 5'-TCGTTGGCTTCGCAACGCTG-3'

ssDNA (150-mer):

5'-CATCTTCCCAGAACCTGGAAACCCTGCAGCCCTGCCCCCATCCGACCTCC
GCCCTCGTTGGCTTCGCAACGCagatctCTCTGTGGCCAGTAGAGGGCACACTTACTTTA
CTTTCACAAATCCGAGAGCCACAACCCGGGTGGTGGGGGG -3'

For mouse genotyping, PCR products amplified using the following primers were digested with *Bgl*II, which replaced each of the native Runx binding sites.

mR1/mR2

5'-GTCGTTCTGGAAAGAATGTGC-3'

5'-GCCCAGTACTCCGGCTCC-3'

mR3

5'-GCAGCCTAAAAGAGTCATTTAAAGG-3'

5'-CCCAAGGCACTTAAAGAAACC-3'

BM-MSCs and mOS and human OS cells

All cells used in this study were confirmed to be free of mycoplasma infection and maintained in F12/DMEM medium supplemented with 10% fetal bovine serum. For generation of BM-MSCs, BM cells were flushed from the femur of 3-month-old mice with F12/DMEM medium. $Cd11b^-$ $Cd45^-$ adherent BM cells, which were negatively selected using a magnetic cell sorting system (MACS) consisting of CD11b and CD45 MicroBeads and MS Columns (Miltenyi Biotec), were used as BM-MSCs. Similarly, for generation of mOS cells, adherent cells obtained from mouse OS tissues that were minced and collagenase I-digested were negatively selected using a MACS. $Cd11b^-$ $Cd45^-$ OS cells were cloned and used as mOS cells. hMSC (human mesenchymal stem cell)/NHOst (human osteoblast cell), U2OS/G292/Saos-2/SJSA1/MNNG-HOS/143B, MG-63/HOS/HuO9, and NOS1 cells were purchased from Lonza, ATCC, JCRB, and RIKEN, respectively.

Immunoblotting and immunoprecipitation

Lysates of OS cells and MSCs for immunoblotting were prepared using a lysis buffer containing 9 M Urea, 2% Triton X-100, 2-mercaptoethanol, and protease/phosphatase inhibitors. OS tissues were homogenized using a FastPrep24 homogenizer (MP Bio). Immunoblotting was performed using the following antibodies: anti-Runx1 (in-house rabbit polyclonal antibody against Runx1 polypeptide MSEALPLGAPDGGAALAS), anti-Runx2 (D1H7; Cell Signaling Technology), anti-Runx3 (D6E2; Cell Signaling Technology), anti-Cbfβ (β-4E8; in-house mouse monoclonal antibody)[1], anti-VWRPY (Rp-6C2; in-house mouse monoclonal antibody), anti-Runx3(P1) (in-house rabbit polyclonal antibody against Runx3(P1) polypeptide SNSIFDSFPNYTPTFIRDP), anti-c-Myc (Y69; Abcam), anti-p53 (DO-1; MBL, 1C12; Cell Signaling Technology), anti-Rb (C-2; Santa Cruz Biotechnology), anti-phosphorylated Rb (Ser780) (D59B7; Cell Signaling Technology), anti-p21 (EPR3993; Abcam), anti-FLAG (M2; Sigma), and anti-β-actin (AC-15; Sigma).

Whole-cell extracts of mOS1-1 cells transiently expressing human wild-type p53 (pcDNA3.1-human p53WT), p53(R156P) (pcDNA3.1-p53R156P), or p53(R273H) (pcDNA3.1-p53R273H) and HEK293T cells transiently expressing human wild-type p53 and RUNX1, 2, or 3

(P1) (pcDNA3.1-RUNX1, 2, or 3-P1) were immunoprecipitated with anti-Runx3 (D6E2) and anti-p53 (DO-1) antibodies as appropriate. The immunoprecipitates from mOS1-1 or HEK293T cells were subjected to immunoblotting using anti-p53 (DO-1)/anti-Runx3 (R3-8C9)[2] antibodies or anti-VWRPY/anti-p53 (FL393; Santa Cruz) antibodies, respectively. The anti-VWRPY antibody was evaluated using whole-cell extracts of HEK293T cells transiently expressing FLAG-tagged full-length Runxs(P1) (pFLAG-CMV-4-Runx1, 2 or 3-P1) or FLAG-tagged full-length Runxs(P1) without VWRPY (pFLAG-CMV-4-Runx1, 2 or 3-P1 ΔVWRPY) and an anti-FLAG antibody. Immunoprecipitates of nuclear extracts (NE) of ST2 cells generated using anti-Runx1, anti-Runx2 (D1H7), or anti-Runx3 (D6E2) antibodies or normal rabbit IgG were subjected to immunoblotting with the anti-VWRPY antibody to confirm the positions of endogenous Runx1, 2, and 3 proteins on the western blotting. To detect endogenous protein interactions, immunoprecipitates of NE of ST2 cells generated using anti-Runx2 (D1H7) or anti-Runx3 (D6E2) antibodies or normal rabbit IgG were subjected to immunoblotting using anti-Runx2 (R2-8G5; MBL), anti-Runx3(R3-8C9), or anti-p53 (1C12) antibodies.

shRNA-knockdown and transplantation

Knockdown of endogenous gene expression was performed using the RNAi-Ready pSIREN-RetroQ Vector (Clontech). Cells were retrovirally transfected and selected with puromycin. Resistant cells were used for subsequent assays without cloning. shRNA sequences targeting *Runx1*, *Runx2*/*RUNX2*, *Runx3*/*RUNX3*, or *Myc*/*MYC* are shown below:

Runx1-1: 5’-AAGACATCGGCAGAAACTAGATGAT-3’
Runx1-2: 5’-AGCTTCACTCTGACCATCA-3’
Runx2/RUNX2-1: 5’-GTTGCAACTGTAAATTGAA-3’
Runx2/RUNX2-2: 5’- GGACTGTGGTTACCGTCAT-3’
Runx3-1: 5’-GGAGCCATATCTCTCTTTC-3’
Runx3-2: 5’-GCATCTCAGTCAAGCATCT-3’
RUNX3-1: 5’-GCCCCAGAGAAGATGAGTCTAT-3’
RUNX3-2: 5’-TCAGTAGTGGGTACCAATCTT-3’
Myc-1: 5’-GAACATCATCATCCAGGAC-3’
MYC-1: 5’-AACAGAAATGTCCTGAGCAAT-3’

Myc/MYC-2: 5’-ACATCATCATCCAGGACTG-3’

Transplantation (xenografts and allografts) was performed by subcutaneous injection of human OS (5×10^6) or mOS (2.5×10^6) cells into 6~8-week-old female BALB/c-*nu/nu* mice (nude mice). Tumorigenicity of OS cells was assessed based on tumor weight 4 weeks after inoculation.

qRT-PCR

Total RNA was extracted using the NucleoSpin RNA kit (Macherey-Nagel) and reverse-transcribed into cDNA using the ReverTra Ace qPCR RT Master Mix (Toyobo). Real-time quantitative PCR reactions were performed on a 7300 Real-time PCR system (ABI) using THUNDERBIRD Probe or SYBR qPCR Mix (Toyobo). The following TaqMan probes (Applied Biosystems) or primer sets were used:

Runx1: Mm00486762_m1

Runx2: Mm03003491_m1

Runx3: Mm00490666_m1 or 5’-ATGAAGAACCAAGTGGCCAGG-3’ and
5’-CTTGATGGCTCGGTGGTAGG-3’

Myc: Mm00487803_m1 or 5’-GTGCTGCATGAGGAGACACC and
5’-CACAGACACCACATCAATTTCTTCC-3’

β-actin: Mm00607939_s1 or 5’-CATCCGTAAAGACCTCTATGCCAAC-3’ and
5’-ATGGAGCCACCGATCCACA-3’

Pvt1: 5’-GTGAAGCGTTGACTTAAGAGATGC-3’ and
5’-TGCAGAACTCAGCTGTCTTATAGG-3’

Digital PCR

Droplet generation and transfer of emulsified samples to PCR plates was performed using a QX200 Droplet Generator (Bio-Rad). Plates were incubated using a thermal cycler with the following conditions: 95°C for 5 min, 40 cycles of 95°C for 30 sec and 60°C for 1 min, 4°C for 5 min, and 90°C for 5 min. Plates were then read on a QX200 Droplet Reader (Bio-Rad), and the data were analyzed using the QuantaSoft Software (Bio-Rad). The following primer pairs were used:

β-actin: 5’-CATCCGTAAAGACCTCTATGCCAAC-3’ and

5’- ATGGAGCCACCGATCCACA-3’

Runx3(P1): 5’-CAAAACAGCAGCCAACCAAGTGG-3’ and

5’-GGTTGGTGTATAGTTGGGGAAGG-3’

Runx3(P2): 5’-TGACGGCCGCGGCATGCGTATTCCC-3’ and

5’-GCTGTTCTCGCCCATCTTGCC-3’

RNA-seq

Two mouse calvariae (OB) were isolated from newborn mice. Seven mouse OS tissues were isolated from seven individual *OS* mice upon OS development. Calvariae and OS tissues were homogenized using a FastPrep24 homogenizer (MP Bio). RNA was extracted from homogenates of these tissue samples using the NucleoSpin RNA kit. RNA quality was assessed on a Bioanalyzer (Agilent). Libraries were prepared using the SureSelect XT RNA Direct System (Agilent) after exome capture was performed using the probe set accompanying the SureSelect XT Mouse All Exon Kit (mm9). Next-generation sequencing (NGS) libraries were sequenced on an MGI-SEQ platform, with an average of 52 million reads and an average mapping rate of 97%. RNA counts were quantified using Kallisto[3] by pseudo-aligning FASTQ reads to the mouse genome (mm10).

RNA-seq data and the corresponding clinical information from 86 primary OS patients (hOS) were obtained from the TARGET project (https://ocg.cancer.gov/programs/target) under accession number phs000468 on NCBI dbGaP. Of those, 83 datasets possessing both sequencing and clinical information were used for downstream analyses. RNA-seq datasets from two human osteoblast (hOB) samples were derived from the ENCODE project under accession number GSE78608. RNA counts were quantified using Kallisto[3] by pseudo-aligning FASTQ reads to the human genome (hg36).

In each of the four groups [mouse (m) OB, mOS, human (h) OB, and hOS], genes were excluded from subsequent analyses if their average expression counts were zero. Principal component analysis (PCA) was performed using the prcomp function of R. Differential expression analysis of OS (mOS, hOS) vs. control osteoblasts (mOB, hOB) was performed using TMM/edgeR in the TCC platform[4], and the results were used to draw both MA plots and heatmaps. The 794 human genes associated with the Gene Ontology term “DNA-templated transcription”

(GO:0000977; https://www.ebi.ac.uk/QuickGO/term/GO:0000977) and the 741 corresponding mouse genes were considered as transcription factors.

Prior to correlation and survival analyses, human gene counts were normalized against the housekeeping gene *ACTB*, which encodes beta-actin. Correlation analysis was performed using Spearman's correlation. Survival analysis was performed, and the hazard ratio was calculated with the Cox proportional hazard model after patients were stratified into low- and high- expressing groups based on the median value for each gene.

Microarrays

Gene expression profiles of BM-MSCs derived from randomly selected 3-month-old *OS* (n=4) and *OS*; *Runx3(P1)*$^{\Delta/\Delta}$ (n=5) mice were assessed by oligonucleotide microarray analysis using the SurePrint G3 Mouse GE Microarray kit 8x60k (Agilent Technologies). Total RNA samples were used for the microarray analyses.

Histological analysis

Tissues were fixed with 4% paraformaldehyde in PBS, decalcified in Osteosoft (Merck Millipore) at room temperature for 10 days, embedded in paraffin, and cut into 4 µm sections. Anti-Myc (Y69, Abcam), anti-Runx2 (Cell Signaling Technology; D1H7), and anti-Runx3 rabbit (Cell Signaling Technology; D6E2) or mouse (R3-8C9) antibodies were used for immunodetection on rehydrated sections pretreated with Target Retrieval Solution (DAKO). The Envision™+ system (HRP/DAB) (DAKO) or Alexa Fluor (488 or 594; Invitrogen) were used for visualization.

Genome editing of OS cells

Mouse mR1 and mR3 were mutated by CRISPR-based genome editing, using the plasmid PX459 (#62988; Addgene). sgRNA sequences were as follows: Scrambled (5'-TGGTTTACATGTCGACTAAC-3'), mR1 (5'-CTGCGTATATCAGTCACCGC-3'), or mR3 (5'-TCGTTGGCTTCGCAACGCTG-3'). Cells were electroporated with the individual plasmids using the Neon Transfection System (Invitrogen).

Human MR1 was mutated by TALEN-based genome editing, using the Platinum Gate TALEN Kit (#1000000043; Addgene). The sequence 5'-TTATACTCACAGGACAAggatgcggtttgtcaaaCAGTACTGCTACGGAGG was used as the target; capital letters indicate sequences recognized by the two corresponding TALEN vectors constructed using the kit. Cells were electroporated with the pair using the Neon Transfection System. Clones harboring the intended mutation were identified by sequencing.

Stable and inducible expression of exogenous genes

Cells were retrovirally transfected with pMSCV-vector (Clontech/Takara), pMSCV-Runx3(P1), pMSCV-RUNX3(P1), or pMSCV-human-p53WT and selected using puromycin. Resistant cells were cloned. Expression of human p53WT, p53(R156P), or p53(R273H) was induced in mOS cells using Retro-X Tet-One Inducible Expression System (Clontech/Takara). mOS cells were retrovirally transfected and selected with puromycin. Resistant cells were cloned and treated with or without 100 ng/ml doxycycline (Dox) for the indicated times.

Luciferase reporter assays

Runx(wt)- or Runx(mt)-Luc vectors harbored 6×Runx wild-type (wt) or mutant (mt) binding sites (wt: 5'-TGCGGTTGCGGTTGCGGTgtcTGCGGTTGCGGTTGCGGT-3'; mt: 5'-TGCCCTTGCCCTTGCCCTgtcTGCCCTTGCCCTTGCCCT-3') between the *Xho*I and *Hin*dIII sites of the pGL4.10[luc2] vector (Promega), respectively. G292 cells were co-transfected with Runx(wt)- or Runx(mt)-Luc and an internal control, pRL-SV40 (Promega), in combination with pcDNA3.1-mock, -human p53WT, -p53(R156P), -p53(R273H), -RUNX2/Runx2(P1), or -RUNX3/Runx3(P1). Transfections were performed using the X-tremeGENE HP DNA Transfection Reagent (Roche). Forty-eight hours after transfection, luciferase activity was measured using the dual-luciferase reporter assay system (Promega).

EMSA

EMSA was performed using the LightShift Chemiluminescent EMSA Kit and Chemiluminescent Nucleic Acid Detection Module (Thermo Scientific). Each binding reaction (10 μl) contained 50 ng/μl poly (dI-dC), 100 fmol labeled probe, and NE in the buffer supplied in the kit. NE was prepared from ST2, MC3T3-E1, and mOS cells, as well as from 293T cells expressing p53 (pcDNA3.1-human p53) or harboring pcDNA3.1, using the NE-PER Nuclear and Cytoplasmic Extraction Reagents (Thermo Fisher Scientific). NE and a labeled DNA probe with or without unlabeled probes were incubated at room temperature for 20 min and resolved on 5% polyacrylamide gels in 0.5x TBE buffer. For super-shift analysis, anti-Runx1, anti-Runx2 (D1H7), or anti-Runx3 (6E2) antibodies or rabbit normal IgG were added after the binding reaction and incubated at room temperature for an additional 10 minutes. NE of p53- or mock-293T cells was incubated on ice for 10 min with NE of mOS1-1 cells, and then for 20 min at room temperature with labeled DNA probe. The following oligonucleotide probes were used: 5'-biotinylated labeled or unlabeled wild-type (wt) mR1, 5'-TTCCACCTGCGGTGACTGAT-3'; 5'-biotinylated labeled T7 or T13, 5'-TTCCACGCGGTGACTGAT-3' or 5'-TTCCACCGGTGACTGAT-3', respectively; and unlabeled mutated (mt) mR1, 5'-TTCCACCTGCCGTGACTGAT-3'.

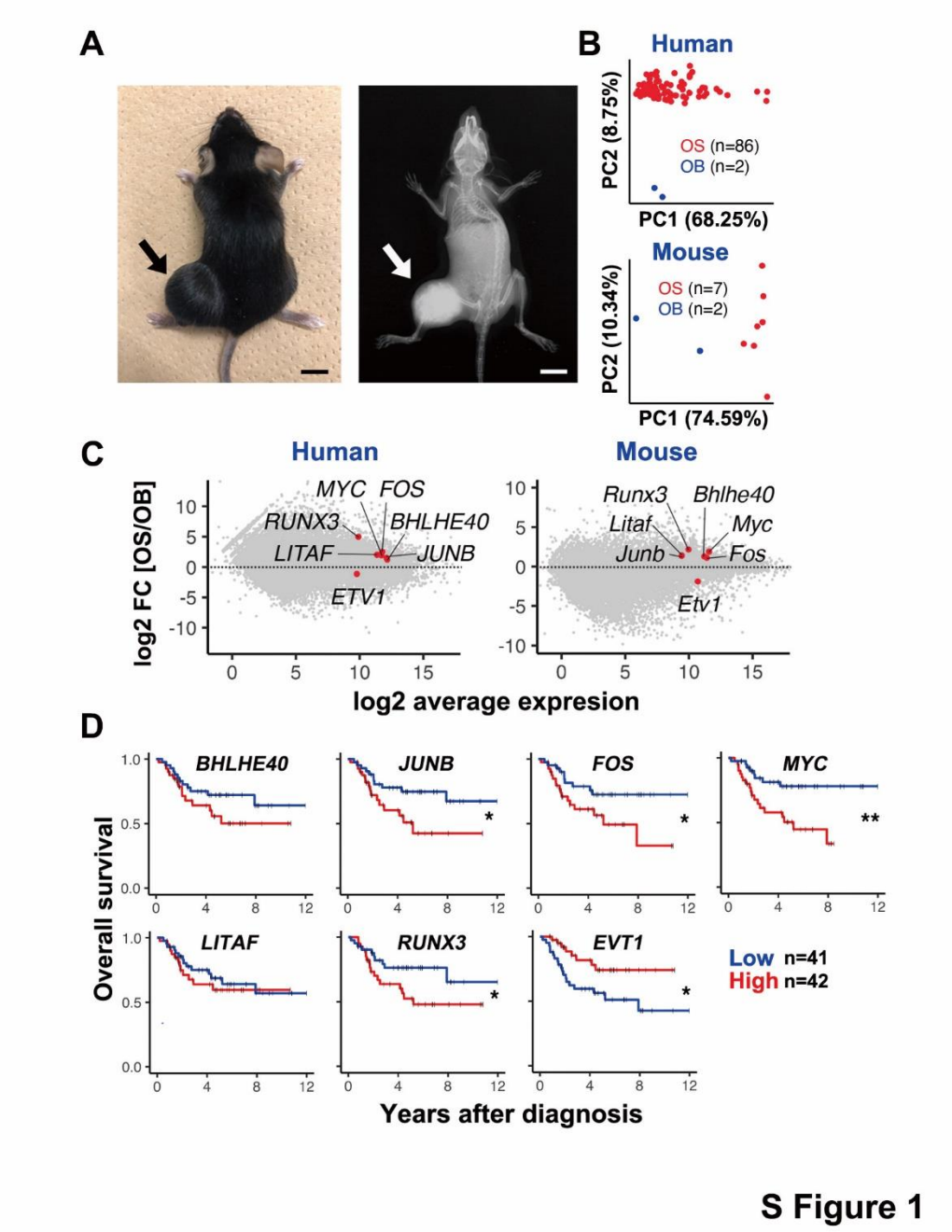

Supplementary Figure 1. Up- and down-regulated transcription factors in *p53*-deficient osteosarcomagenesis in human and mouse.

(A) OS development in the tibia of a representative osteoprogenitor-specific *p53* knockout mouse (*Osterix/Sp7*-Cre; $p53^{fl/fl}$). Arrows indicate the tumor. *Osterix*-Cre is expressed in BM-MSCs of adult mice as well[5]. Right panel: radiograph. A scale bar = 1 cm. (B) Principal component analysis (PCA) of RNA-seq data comparing OS tissues (OS) and normal osteoblasts (OB) in human and mouse. (C) MA plot presentation of RNA-seq data comparing OS and OB. The seven TFs (Fig. 1A, B) are indicated by red dots. (D) Prognostic efficacy of the seven transcription factors (Fig. 1A, B) as determined by Kaplan–Meier analysis of survival in the OS patients in the TARGET cohort. $^{**}p < 0.01$; $^{*}p < 0.05$.

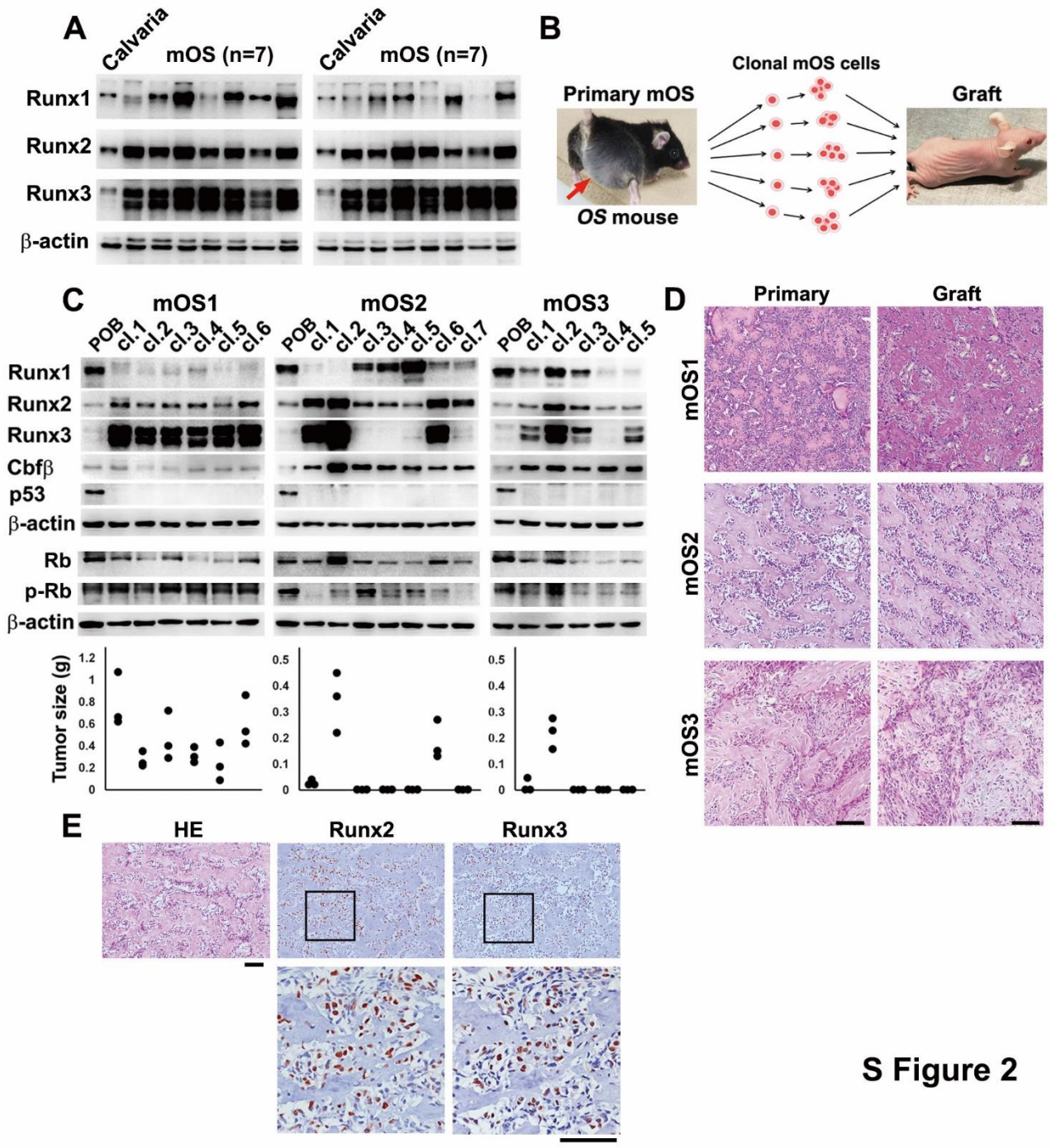
A
Calvaria
mOS (n=7)
Calvaria
mOS (n=7)
Runx1
Runx2
Runx3
β-actin
B
Primary mOS
Clonal mOS cells
Graft
OS mouse
C
mOS1
mOS2
mOS3
POB
cl.1
cl.2
cl.3
cl.4
cl.5
cl.6
cl.7
Runx1
Runx2
Runx3
Cbfβ
p53
β-actin
Rb
p-Rb
β-actin
Tumor size (g)
D
Primary
Graft
mOS1
mOS2
mOS3
E
HE
Runx2
Runx3

S Figure 2

Supplementary Figure 2. Runx3 is required for tumorigenicity of *p53*-deficient OS.
(A) Levels of the indicated proteins in OS (mOS) in 14 individual *OS* mice and newborn calvaria, as determined by western blotting. (B) Tumorigenicity of clonal mOS cells isolated from mOS (arrow) in individual *OS* mice (left) was evaluated by allograft in nude mice (BALB/c *nu/nu* mice; right). (C) Levels of the indicated proteins in clonal OS cells isolated from OS (mOS1~3) in three individual *OS* mice, and primary osteoblasts (POB) derived from newborn calvaria, as determined by western blotting (upper). The tumorigenicity of each clone was evaluated by allograft (lower; n=3). Clone 1 of mOS1 and clone 2 of mOS2 were used as mOS1-1 and mOS2-2 cells, respectively, in this study. (D) Strong histological similarity of primary OS (mOS1–3) in three individual *OS* mice (Primary; left panels) and allograft OS of mOS1 clone 1, mOS2 clone 2, and mOS3 clone 2 (grafts; top right, middle right, and bottom right, respectively). (E) Representative histology of OS in *OS* mice (HE; left) and immunodetection of Runx2 and Runx3 (center and right). Serial sections were used. Boxed regions are enlarged below. Counter staining was done with hematoxylin. Scale bars = 100 μm.

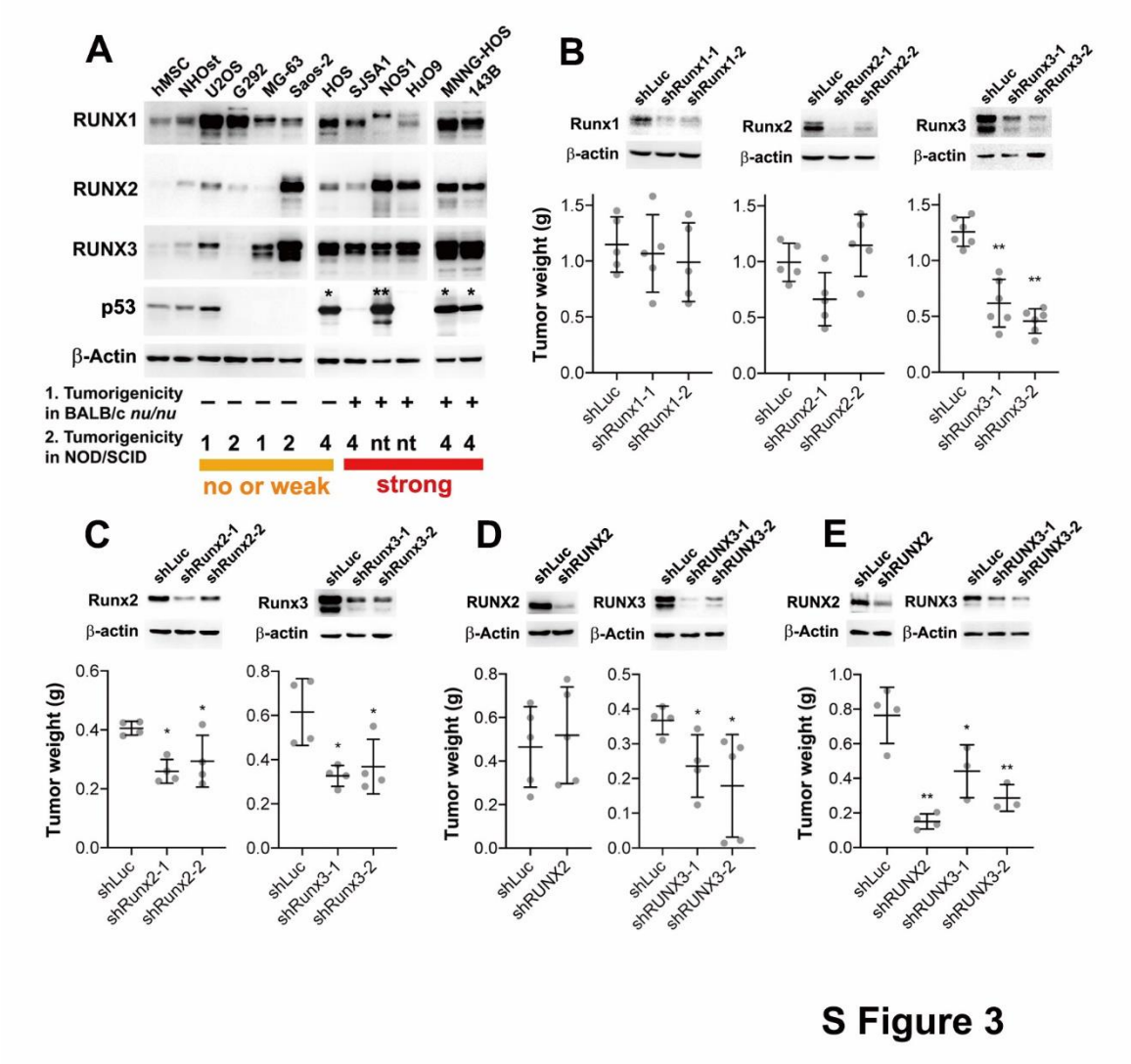

S Figure 3

Supplementary Figure 3. RUNX3/Runx3 is required for tumorigenicity of human and mouse *p53*-deficient OS.

(A) Expression profile of the indicated proteins in human OS cell lines, normal human MSC (hMSC), and osteoblast (NHOst), as determined by western blotting. Tumorigenicity of the human OS cell line was classified based on previously published results [1[6] and 2[7]. NOS1 and HuO9 were also tumorigenic in xenografts using BALB/c *nu/nu* mice as reported[8] and shown in (E), respectively. Mutated p53s are indicated by asterisks: *R156P and **R273H (Supplementary Fig. 11E). nt, not tested. (B) Effects of knockdown of Runx1, Runx2, or Runx3 on tumorigenicity of mOS1-1 cells (mOS1 cl.1 cells shown in Supplementary Fig. 2C). Levels of the indicated proteins in cells, as determined by western blotting (upper). Tumorigenicity was evaluated by allograft (lower). (C) Effects of knockdown of Runx2 or Runx3 on tumorigenicity of mOS2-2 cells (mOS2 cl.2 cells shown in Supplementary Fig. 2C). Levels of the indicated proteins in the cells were determined by western blotting (upper). Tumorigenicity was evaluated by allograft (lower). (D and E) Effects of knockdown of RUNX2 or RUNX3 on tumorigenicity of SJSA1 (D) and HuO9 (E) cells. Levels of the indicated proteins in the cells were determined by western blotting (upper). Tumorigenicity was evaluated by xenograft (lower). $^{**}p < 0.01$; $^{*}p < 0.05$.

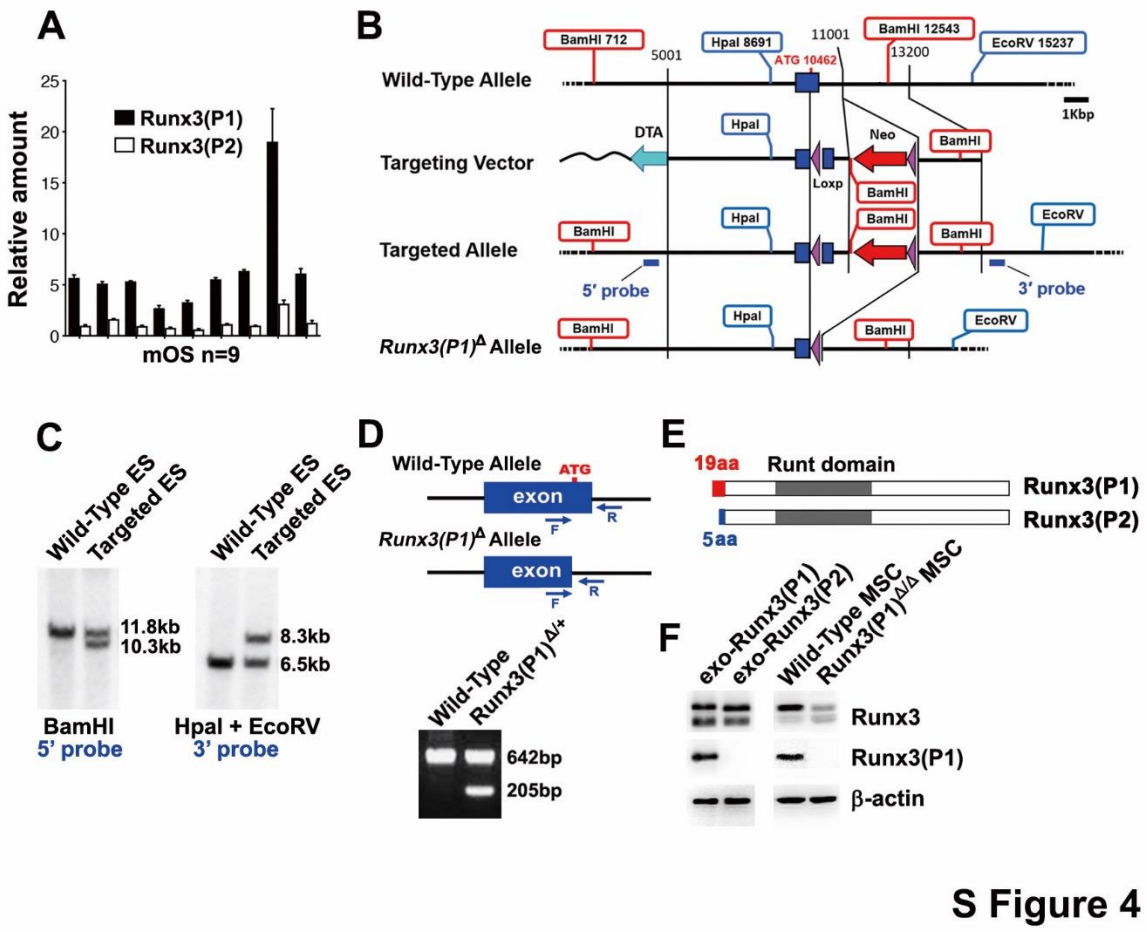

S Figure 4

Supplementary Figure 4. Generation of *Runx3(P1)*-deleted mice.
(A) Levels of mRNA of *Runx3(P1)* and *Runx3(P2)* in nine OS (mOS) developed in nine individuals of *OS* mice, as determined by digital PCR (n=3). (B) Targeting vector for homologous recombination and strategy for generating the *Runx3(P1)*-deleted mouse line. (C) Southern blot analyses of genomic DNA of wild-type and targeted ES cells digested with *BamHI* (left) or *HpaI* and *EcoRV* (right) using 5' or 3' probes shown in (B), respectively. (D) Genotyping PCR for detection of wild-type and *Runx3(P1)*$^{\Delta}$ alleles using F and R primers. (E) Structure of Runx3(P1) and Runx3(P2) proteins. The distinct N-terminal amino acids of Runx3 (P1) and Runx3 (P2) are (M)ASNSIFDSFPNYTPTFIR (19 aa) and (M)RIPV (5 aa), respectively. (F) Runx3(P1) was not expressed in BM-MSCs of *Runx3(P1)*$^{\Delta/\Delta}$ mice, as determined by western blotting with an anti-Runx3(P1)-specific antibody (right). Whole-cell extracts of HEK293T cells exogenously expressing Runx3(P1) or Runx3(P2) were subjected to western blotting (left).

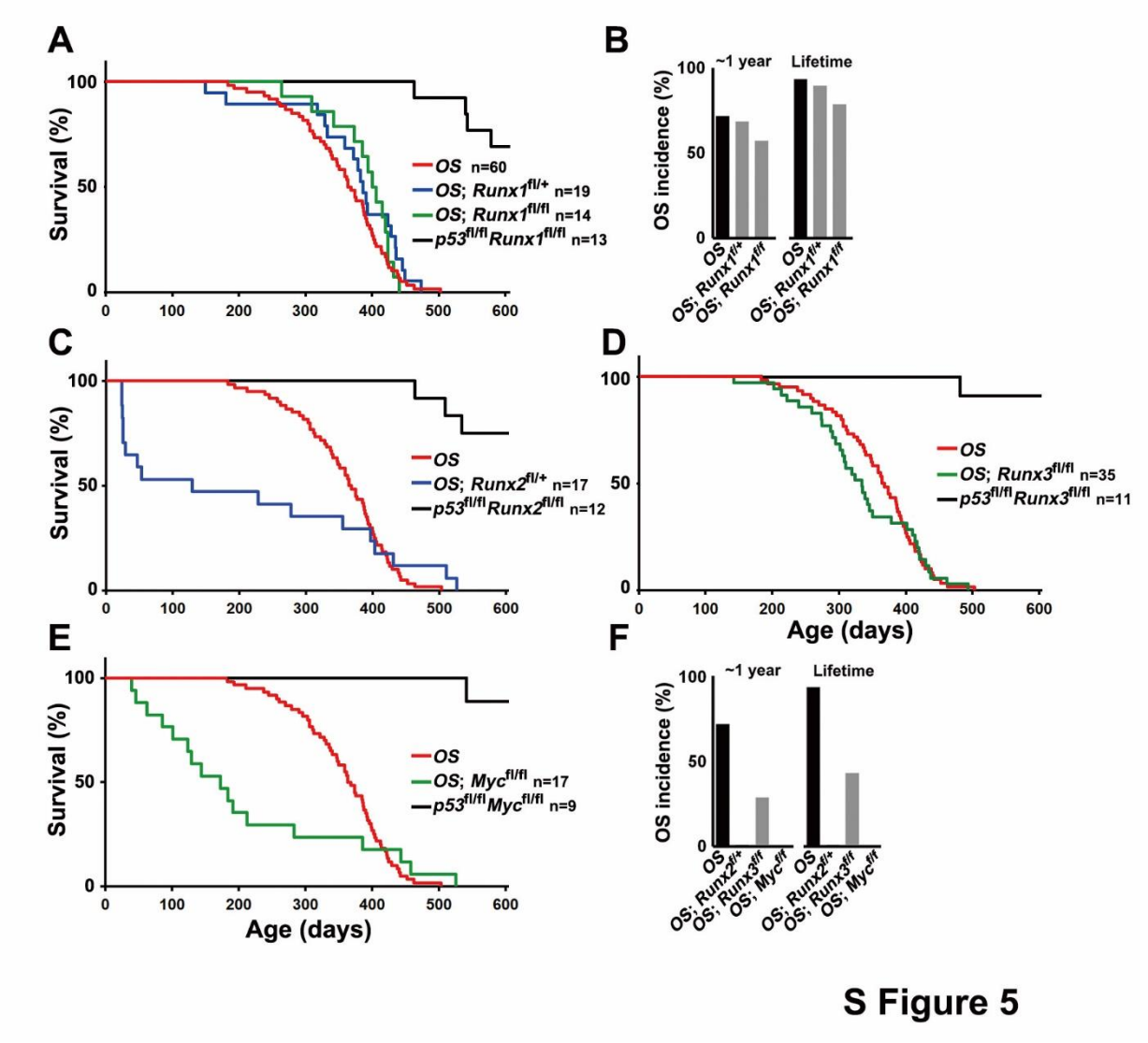

S Figure 5

Supplementary Figure 5. Effects of heterozygous knockout of *Runx1* or *Runx2* and homozygous knockout of *Runx1*, *Runx3*, or *Myc* on *OS* mice.
(A) Survival of the indicated mouse lines. $p53^{fl/fl}Runx1^{fl/fl}$ line is a Cre-free control. (B) OS incidence in the mouse lines shown in (A) within 1 year and throughout the lifespan. (C) Survival of the indicated mouse lines. $p53^{fl/fl}Runx2^{fl/fl}$ line is a Cre-free control. (D) Survival of the indicated mouse lines. $p53^{fl/fl}Runx3^{fl/fl}$ line is a Cre-free control. (E) Survival of the indicated mouse lines. $p53^{fl/fl}Myc^{fl/fl}$ line is a Cre-free control. (F) OS incidence in the mouse lines shown in (C) to (E) within 1 year and throughout the lifespan. In *OS*; $Runx2^{fl/+}$ and *OS*; $Myc^{fl/fl}$ mice, no OS was observed. The results of *OS* mice are identical to those in Fig. 1D, E (A−F).

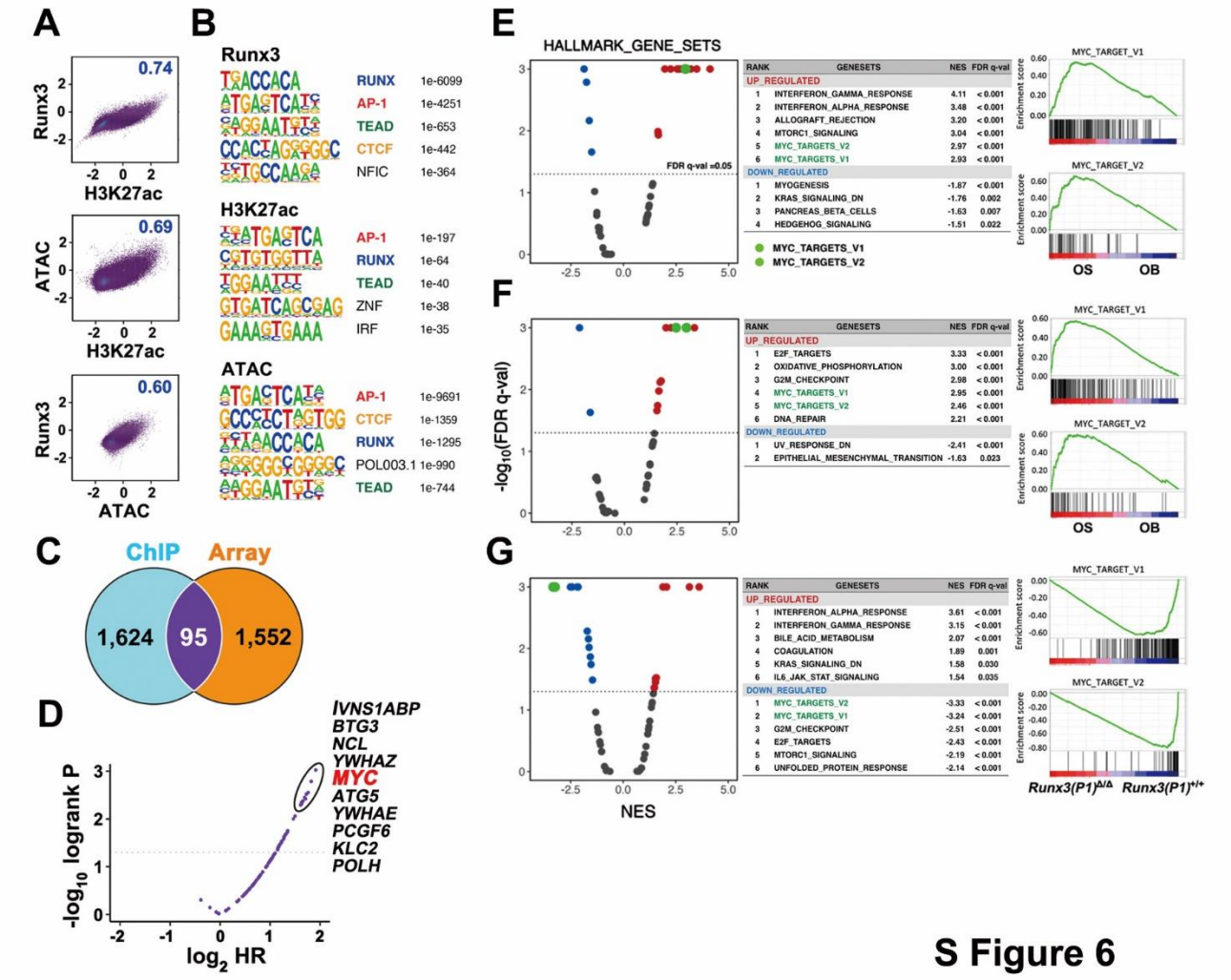

Supplementary Figure 6. Identification of target genes upregulated by Runx3, a transcriptional activator, in *p53*-deficient mOS cells.

(A) Genome-wide correlations among the profiles of Runx3 and H3K27ac ChIP-seq and ATAC-seq (Fig. 2A). Pearson correlation coefficient is shown in each panel. (B) Enriched consensus motif of transcription factors in the genome-wide profiles of Runx3 and H3K27ac ChIP-seq and ATAC-seq. (C) Number of genes upregulated by Runx3 in BM-MSCs (Array) or bound by Runx3 in mOS cells (ChIP). The 95 overlapping genes, listed in Supplemental Table S2, were considered as Runx3 target genes in this study. (D) Volcano plot of the hazard ratio values for the 95 Runx3 target genes, as calculated based on the TARGET data. Myc was among the factors most strongly associated with poor prognosis (circled). (E-G) Gene set enrichment analyses using Hallmark Gene Sets and the following transcriptome datasets: RNA-seq data from mouse OS tissues compared with non-tumor OBs (E); RNA-seq data from human OS tissues compared with non-tumor OBs (F); and microarray data from either *Runx3(P1)*$^{\Delta/\Delta}$ or *Runx3(P1)*$^{+/+}$ *p53*-null BM-MSCs (G). Shown for each analysis are the following: a volcano plot representing normalized-enrichment scores (NES) on the x-axis for the overall result (left); a list of the six most significantly up- and down-regulated gene sets (middle); and an individual enrichment graph of Myc-target genes (right).

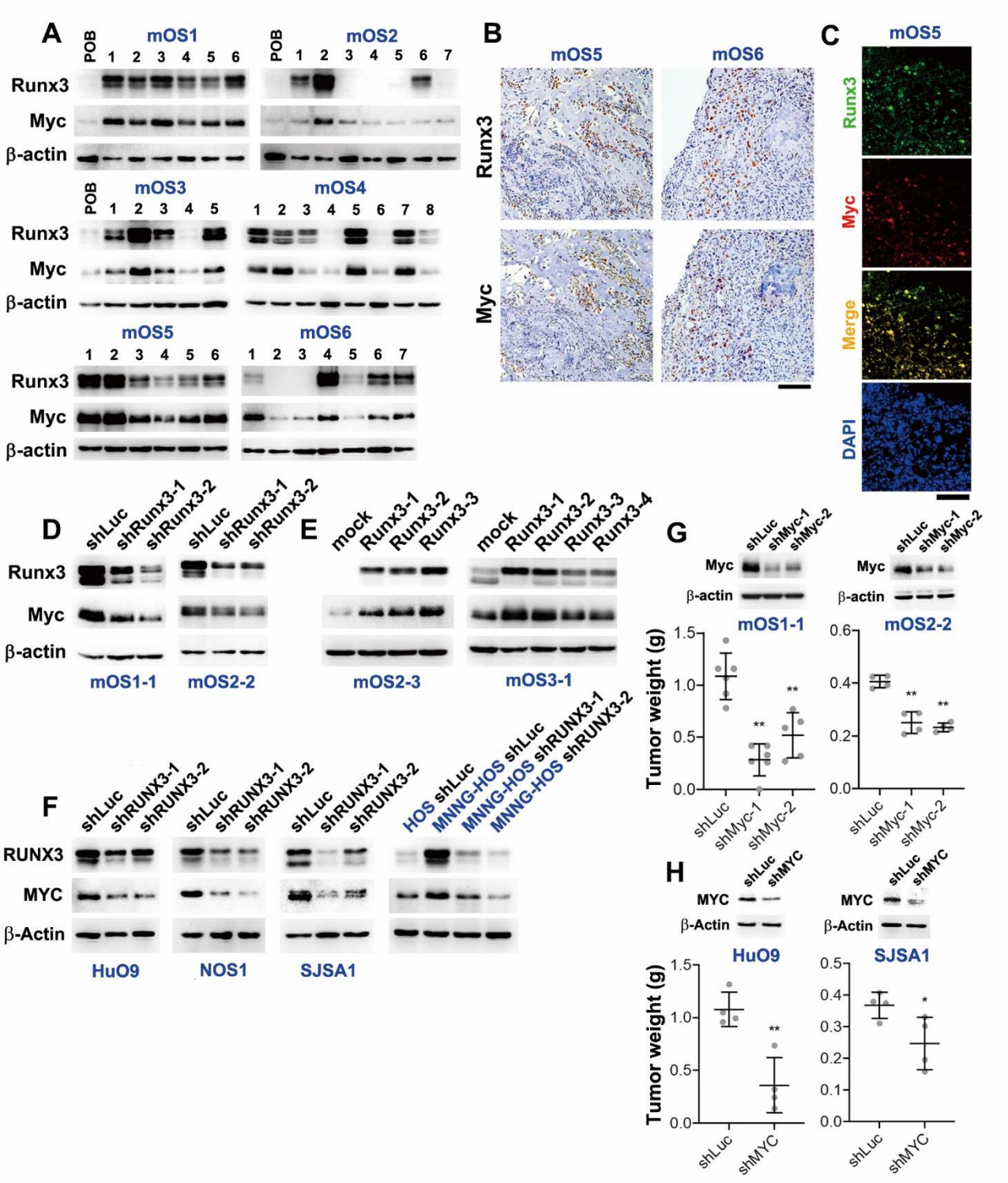
A
POB
mOS1
1 2 3 4 5 6
mOS2
1 2 3 4 5 6 7
Runx3
Myc
β-actin
mOS3
1 2 3 4 5
mOS4
1 2 3 4 5 6 7 8
mOS5
1 2 3 4 5 6
mOS6
1 2 3 4 5 6 7
B
mOS5
mOS6
Runx3
Myc
C
mOS5
Runx3
Myc
Merge
DAPI
D
shLuc
shRunx3-1
shRunx3-2
mOS1-1
mOS2-2
E
mock
Runx3-1
Runx3-2
Runx3-3
Runx3-4
mOS2-3
mOS3-1
F
shLuc
shRUNX3-1
shRUNX3-2
HOS shLuc
MNNG-HOS shLuc
MNNG-HOS shRUNX3-1
MNNG-HOS shRUNX3-2
RUNX3
MYC
β-Actin
HuO9
NOS1
SJSA1
G
shLuc
shMyc-1
shMyc-2
Myc
β-actin
mOS1-1
mOS2-2
Tumor weight (g)
H
shLuc
shMYC
MYC
β-Actin
HuO9
SJSA1
Tumor weight (g)

S Figure 7

Supplementary Figure 7. High correlation between Runx3 and Myc levels in *p53*-deficient OS.

(A) Amounts of Runx3 and Myc in clonal OS cells derived from primary OS (mOS1–6) developed in six individual *OS* mice, as determined by western blotting. Clonal OS cells derived from mOS1–3 were also used in Supplementary Fig. 2C. (B) Immunodetection of Runx3 and Myc in mOS5 and mOS6. Upper and lower panels show serial sections. Counterstaining was performed with hematoxylin. Scale bar = 100 μm. (C) Co-immunodetection of Runx3 (green) and Myc (red) in mOS5. Nuclei were visualized with DAPI. Scale bar = 50 μm. (D) Effect of knockdown of Runx3 on expression of Myc in mOS1-1 (clone 1 of mOS1) and mOS2-2 (clone 2 of mOS2) cells, as determined by western blotting. (E) Effects of Runx3 overexpression on Myc expression in mOS2-3 (clone 3 of mOS2) and mOS3-1 (clone 1 of mOS3) cells, as determined by western blotting. (F) Effects of knockdown of RUNX3 on MYC expression in human OS cell lines HuO9, NOS1, SJSA1, and MNNG-HOS, as determined by western blotting. (G) Effects of knockdown of Myc on tumorigenicity of mOS1-1 and mOS2-2 cells. Levels of the indicated proteins in the cells were determined by western blotting (upper), and tumorigenicity was evaluated by allograft (lower). (H) Knockdown effects of MYC on tumorigenicity of HuO9 and SJSA1 cells. Levels of the indicated proteins in the cells were determined by western blotting (upper), and tumorigenicity was evaluated by xenograft (lower). $^{**}p < 0.01$; $^{*}p < 0.05$.

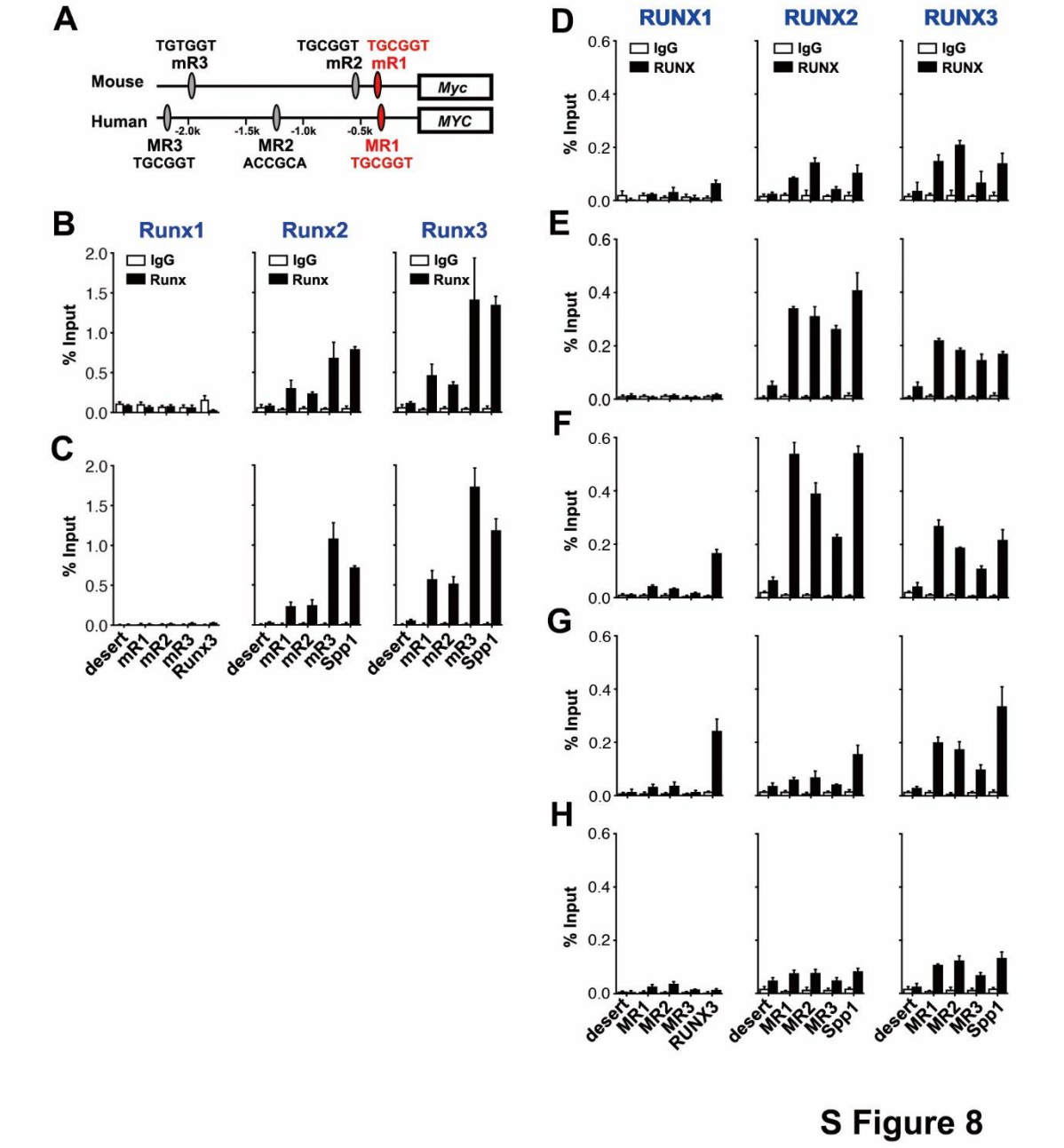

S Figure 8

Supplementary Figure 8. Occupancy of Runx proteins in the *Myc/MYC* promoter.
(A) Runx/RUNX consensus binding sites, mR1/MR1, mR2/MR2, and mR3/MR3 in the *Myc/MYC* promoter. (B and C) Occupancy of Runx1–3 on mR1–3 in mOS1-1 (B) and mOS2-2 (C) cells, as assessed by ChIP. (D−H) Occupancy of RUNX1-3 on MR1-3 assessed by ChIP in SJSA1 (D), NOS1 (E), HuO9 (F), MNNG-HOS (G), and 143B (H) cells. A Runx consensus site in the *Runx3(P1)* promoter (RUNX3)[9] and the *Spp1* promoter (Spp1)[10] were used as positive controls for Runx1 and Runx2/3 ChIP, respectively, and a gene-desert region of the mouse genome (desert) was used as a negative control for all ChIP assays (B−H) (n=3).

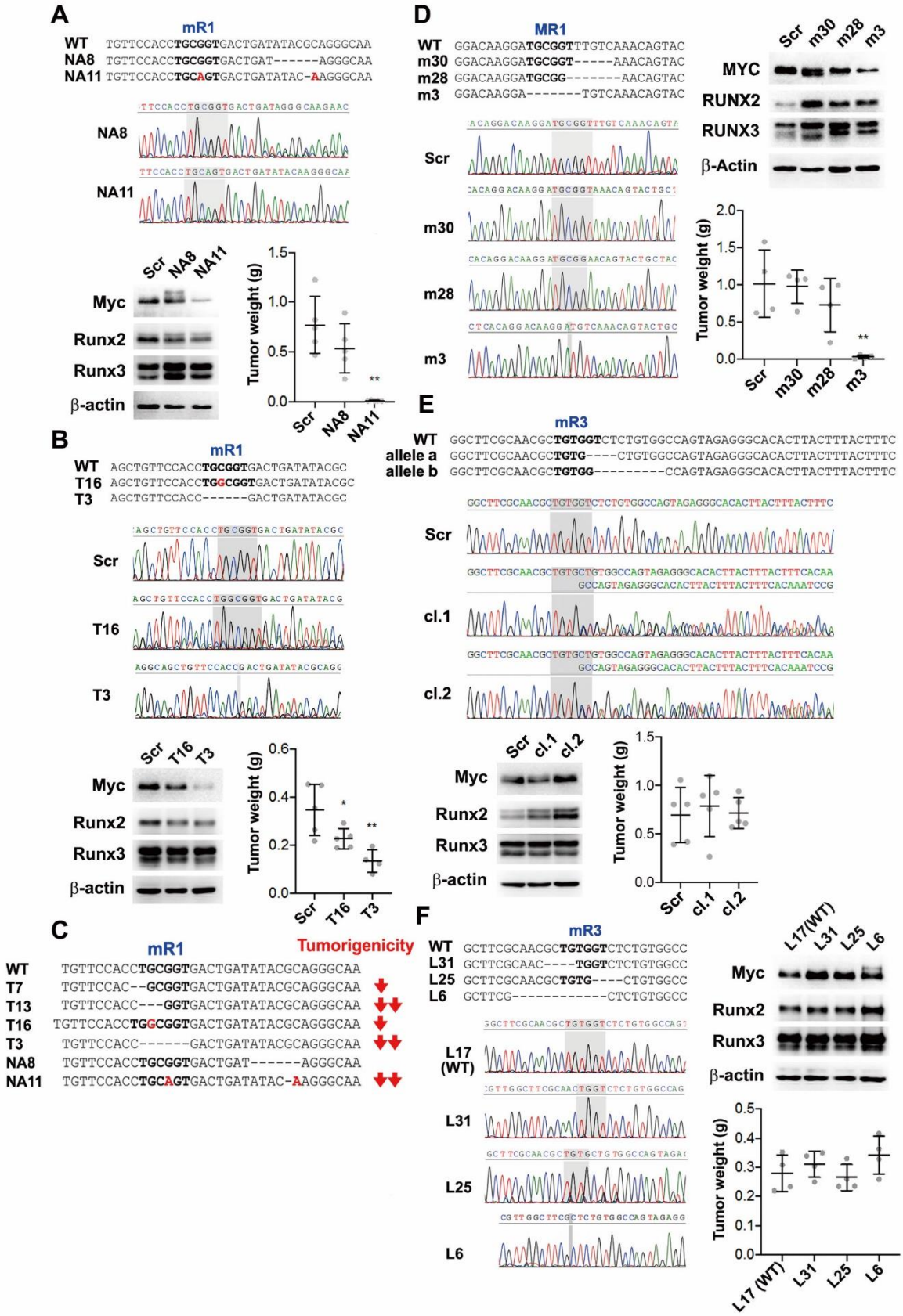
A
mR1
WT TGTTCCACCTGCGGTGACTGATATACGCAGGGCAA
NA8 TGTTCCACCTGCGGTGACTGAT------AGGGCAA
NA11 TGTTCCACCTGCAGTGACTGATATAC-AAGGGCAA
NA8
NA11
Scr NA8 NA11
Myc
Runx2
Runx3
β-actin
Tumor weight (g)
Scr NA8 NA11
B
mR1
WT AGCTGTTCCACCTGCGGTGACTGATATACGC
T16 AGCTGTTCCACCTGGCGGTGACTGATATACGC
T3 AGCTGTTCCACC------GACTGATATACGC
Scr
T16
T3
Scr T16 T3
Myc
Runx2
Runx3
β-actin
Tumor weight (g)
Scr T16 T3
C
mR1
Tumorigenicity
WT TGTTCCACCTGCGGTGACTGATATACGCAGGGCAA
T7 TGTTCCAC--GCGGTGACTGATATACGCAGGGCAA
T13 TGTTCCACC---GGTGACTGATATACGCAGGGCAA
T16 TGTTCCACCTGGCGGTGACTGATATACGCAGGGCAA
T3 TGTTCCACC------GACTGATATACGCAGGGCAA
NA8 TGTTCCACCTGCGGTGACTGAT------AGGGCAA
NA11 TGTTCCACCTGCAGTGACTGATATAC-AAGGGCAA
D
MR1
WT GGACAAGGATGCGGTTTGTCAAACAGTAC
m30 GGACAAGGATGCGGT-----AAACAGTAC
m28 GGACAAGGATGCGG-------AACAGTAC
m3 GGACAAGGA-------TGTCAAACAGTAC
Scr
m30
m28
m3
Scr m30 m28 m3
MYC
RUNX2
RUNX3
β-Actin
Tumor weight (g)
Scr m30 m28 m3
E
mR3
WT GGCTTCGCAACGCTGTGGTCTCTGTGGCCAGTAGAGGGCACACTTACTTTACTTTC
allele a GGCTTCGCAACGCTGTG----CTGTGGCCAGTAGAGGGCACACTTACTTTACTTTC
allele b GGCTTCGCAACGCTGTGG---------CCAGTAGAGGGCACACTTACTTTACTTTC
Scr
cl.1
cl.2
Scr cl.1 cl.2
Myc
Runx2
Runx3
β-actin
Tumor weight (g)
Scr cl.1 cl.2
F
mR3
WT GCTTCGCAACGCTGTGGTCTCTGTGGCC
L31 GCTTCGCAAC----TGGTCTCTGTGGCC
L25 GCTTCGCAACGCTGTG----CTGTGGCC
L6 GCTTCG----------CTCTGTGGCC
L17 (WT)
L31
L25
L6
L17(WT) L31 L25 L6
Myc
Runx2
Runx3
β-actin
Tumor weight (g)
L17 (WT) L31 L25 L6

S Figure 9

Supplementary Figure 9. mR1 is required for tumorigenicity of *p53*-deficient OS cells.
(A) Sequence alignments of genome-edited mOS1-1 cells, NA8 and NA11, bearing homozygous indels around or within mR1. Levels of the indicated proteins in Scr, NA8, and NA11 mOS1-1 cells were determined by western blotting; tumorigenicity of each cell line is shown. (B) Sequence alignments of genome-edited mOS2-2 cells, T16 and T3, bearing homozygous indels in mR1 and the control cells (Scr). Levels of the indicated proteins in Scr, T16, and T3 mOS2-2 cells were determined by western blotting, and the tumorigenicity of each cell line is shown. (C) Summary of reduction in tumorigenicity of mOS cells caused by indels around or within mR1 shown in (A), (B), and Fig. 3G, J. More or less than 50% reduction in tumorigenicity relative to the control is indicated by two downward arrows or one downward arrow, respectively. (D) Sequence alignments of genome-edited SJSA1 cells, m30, m28, and m3, bearing homozygous indels around or within MR1, and control cells (Scr). Levels of the indicated proteins in Scr, m30, m28, and m3 SJSA1 cells were determined by western blotting, and tumorigenicity of each cell line is shown. (E) Sequence alignments of genome-edited mOS1-1 cells, clones 1 and 2, both bearing the same pair of alleles (a and b) with indels around or within mR3, and the control cells (Scr). Levels of the indicated proteins in Scr and clones 1 and 2 mOS1-1 cells were determined by western blotting, and tumorigenicity of each cell line is shown. (F) Sequence alignments of genome-edited mOS2-2 cells, L31, L25, and L6, bearing homozygous genetic alterations around or within mR3 and the control cells bearing intact mR3 (L17). Levels of the indicated proteins in L17, L31, L25, and L6 mOS2-2 cells were determined by western blotting, and the tumorigenicity of each cell line is shown. $^{**}p < 0.01$; $^{*}p < 0.05$.

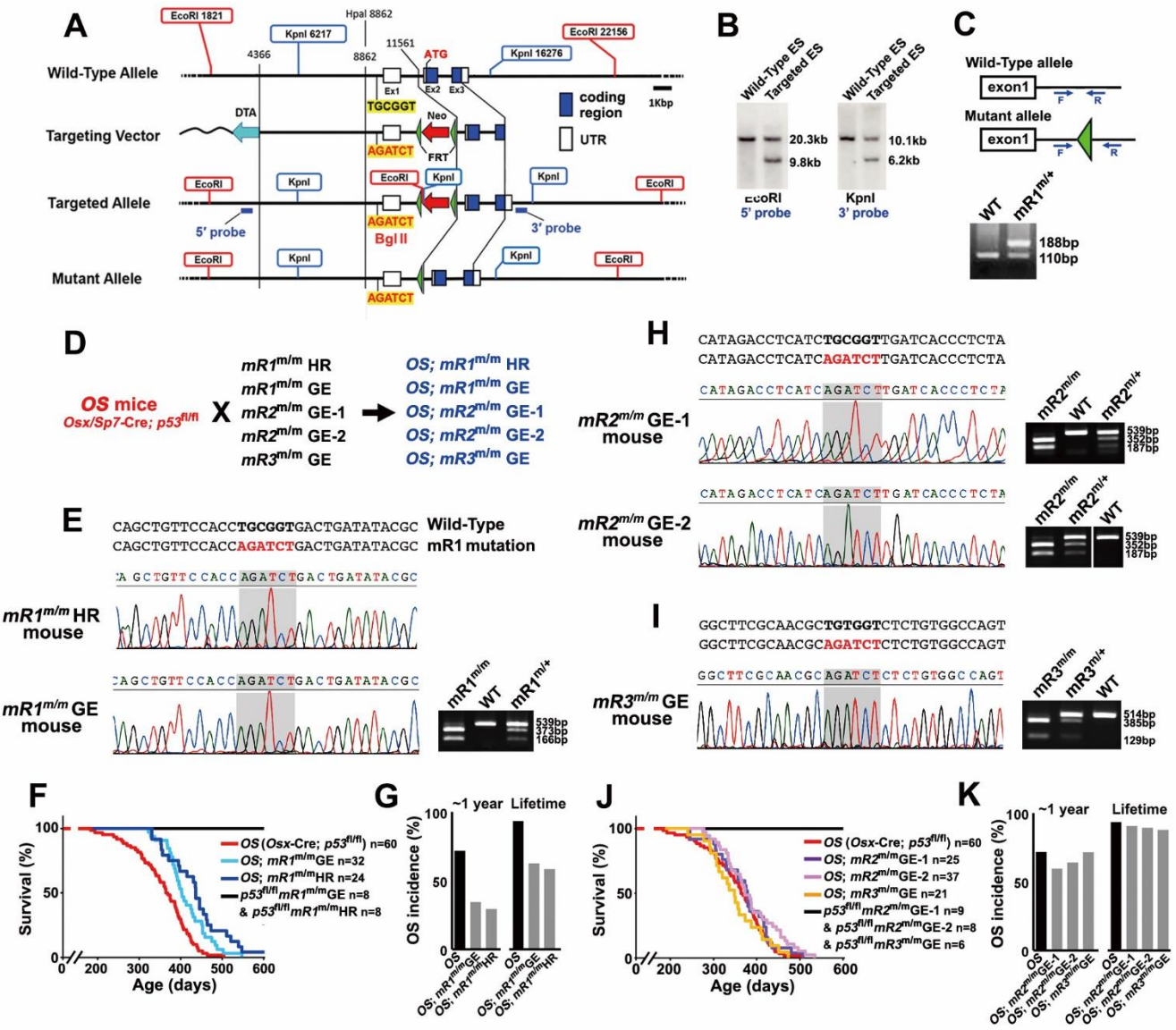
A
EcoRI 1821
KpnI 6217
HpaI 8862
4366
8862
11561
ATG
KpnI 16276
EcoRI 22156
Wild-Type Allele
Ex1
Ex2
Ex3
TGCGGT
coding region
1Kbp
DTA
Targeting Vector
Neo
AGATCT
FRT
UTR
Targeted Allele
EcoRI
KpnI
5' probe
3' probe
BglII
Mutant Allele
B
Wild-Type ES
Targeted ES
20.3kb
9.8kb
10.1kb
6.2kb
EcoRI
5' probe
KpnI
3' probe
C
Wild-Type allele
exon1
F
R
Mutant allele
WT
mR1m/+
188bp
110bp
D
OS mice
Osx/Sp7-Cre; p53fl/fl
X
mR1m/m HR
mR1m/m GE
mR2m/m GE-1
mR2m/m GE-2
mR3m/m GE
OS; mR1m/m HR
OS; mR1m/m GE
OS; mR2m/m GE-1
OS; mR2m/m GE-2
OS; mR3m/m GE
E
CAGCTGTTCCACCTGCGGTGACTGATATACGC Wild-Type
CAGCTGTTCCACCAGATCTGACTGATATACGC mR1 mutation
mR1m/m HR mouse
mR1m/m GE mouse
mR1m/m
WT
mR1m/+
539bp
373bp
166bp
H
CATAGACCTCATCTGCGGTTGATCACCCTCTA
CATAGACCTCATCAGATCTTGATCACCCTCTA
mR2m/m GE-1 mouse
mR2m/m GE-2 mouse
mR2m/m
WT
mR2m/+
539bp
352bp
187bp
I
GGCTTCGCAACGCTGTGGTCTCTGTGGCCAGT
GGCTTCGCAACGCAGATCTCTCTGTGGCCAGT
mR3m/m GE mouse
mR3m/m
mR3m/+
WT
514bp
385bp
129bp
F
Survival (%)
Age (days)
OS (Osx-Cre; p53fl/fl) n=60
OS; mR1m/mGE n=32
OS; mR1m/mHR n=24
p53fl/flmR1m/mGE n=8
& p53fl/flmR1m/mHR n=8
G
~1 year
Lifetime
OS incidence (%)
OS
OS; mR1m/mGE
OS; mR1m/mHR
J
Survival (%)
Age (days)
OS (Osx-Cre; p53fl/fl) n=60
OS; mR2m/mGE-1 n=25
OS; mR2m/mGE-2 n=37
OS; mR3m/mGE n=21
p53fl/flmR2m/mGE-1 n=9
& p53fl/flmR2m/mGE-2 n=8
& p53fl/flmR3m/mGE n=6
K
~1 year
Lifetime
OS incidence (%)
OS
OS; mR2m/mGE-1
OS; mR2m/mGE-2
OS; mR3m/mGE

S Figure 10

Supplementary Figure 10. mR1 is required for tumorigenicity of *OS* mice.
(A) Targeting vector for homologous recombination and strategy for generating an mR1-mutated mouse line by *BglII* substitution. (B) Southern blot analyses of genomic DNA of wild-type and targeted ES cells digested with *EcoRI* (left) or *KpnI* (right) using the 5' or 3' probes shown in (**A**), respectively. (C) Genotyping PCR for detection of wild-type and mutated alleles using F and R primers. (D) Generation of *OS; mR1*$^{m/m}$, *OS; mR2*$^{m/m}$, and *OS; mR3*$^{m/m}$ mice. Two independent mouse lines were prepared for each of *mR1*$^{m/m}$ and *mR2*$^{m/m}$. One *mR1*$^{m/m}$ line (*mR1*$^{m/m}$ HR) was generated using homologous recombination, as shown in (A−C), and the other *mR1*$^{m/m}$ line (*mR1*$^{m/m}$ GE), two *mR2*$^{m/m}$ lines (*mR2*$^{m/m}$ GE-1 and -2), and the *mR3*$^{m/m}$ line (*mR3*$^{m/m}$ GE) were generated by genome editing. (E) Replacement of mR1 with a *BglII* site in *mR1*$^{m/m}$ HR and GE mice, as confirmed by sequencing. Digestion of 539 bp amplified DNA from the mutant allele with *BglII* produces 373 bp and 166 bp DNA fragments. (F) Survival of the indicated mouse lines. *p53*$^{fl/fl}$*mR1*$^{m/m}$ GE and HR lines are Cre-free controls. (G) OS incidence in the mouse lines shown in (F) within 1 year and throughout the lifespan. The results for *OS* mice are identical to those in Fig. 1D or E. (H) Replacement of mR2 with a *BglII* site in *mR2*$^{m/m}$ GE-1 and -2 mice, as confirmed by sequencing. Digestion of the 539 bp DNA amplified from the mutant allele with *BglII* produces 352 bp and 187 bp DNA fragments. (I) Replacement of mR3 with a *BglII* site in *mR3*$^{m/m}$ GE mice, as confirmed by sequencing. Digestion of the 514 bp DNA amplified from the mutant allele with *BglII* produces 385 bp and 129 bp DNA fragments. (J) Survival of the indicated mouse lines. *p53*$^{fl/fl}$*mR2*$^{m/m}$ GE-1, -2, and *p53*$^{fl/fl}$*mR3*$^{m/m}$ GE lines are Cre-free controls. (K) OS incidence in the mouse lines shown in (J) within 1 year and throughout the lifespan. The results of *OS* mice are identical to those in Fig. 1D or E.

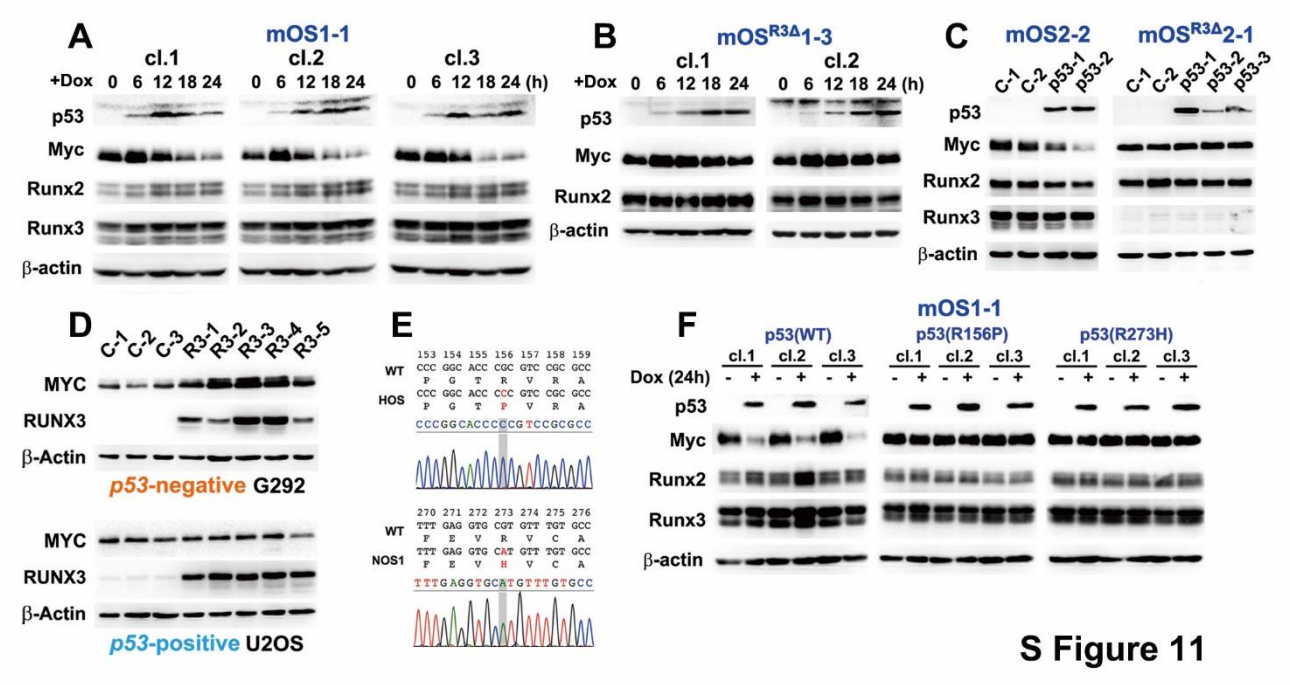

Supplementary Figure 11. p53 attenuates Myc upregulation by Runx3.
(A) Repression of Myc by restoration of p53 induced by doxycycline (Dox) in three clonal mOS1-1 cells (cl. 1–3). Levels of the indicated proteins in the cells were determined by western blotting. (B) Myc was not significantly repressed by restoration of p53 induced by Dox in two clonal mOS$^{R3\Delta}$1–3 cells (cl. 1 and 2), which are *Runx3*-negative (Supplementary Fig. 13A, C). Levels of the indicated proteins were determined by western blotting. (C) Repression of Myc by restoration of stable p53 in mOS2-2 cells, but not in mOS$^{R3\Delta}$2-1 *Runx3*-negative cells (Supplementary Fig. 13A). (D) Levels of the indicated proteins in stable mock (C)- or RUNX3 (R3)-clonal transfectants of *p53*-negative G292 or -positive U2OS cells, as determined by western blotting. (E) *TP53* mutations, R156P and R273H, revealed by sequencing of cDNAs expressed in HOS and NOS1 cells, respectively. R156P is inherited in two HOS derivatives, MNNG-HOS and 143B lines, as indicated in the IARC TP53 Database (https://p53.iarc.fr/celllines.aspx). (F) Myc was not significantly repressed by the p53(R156P) or p53(R273H) mutants induced by Dox in mOS1-1 cells. Three independent clonal cells (cl. 1–3) were used for each.

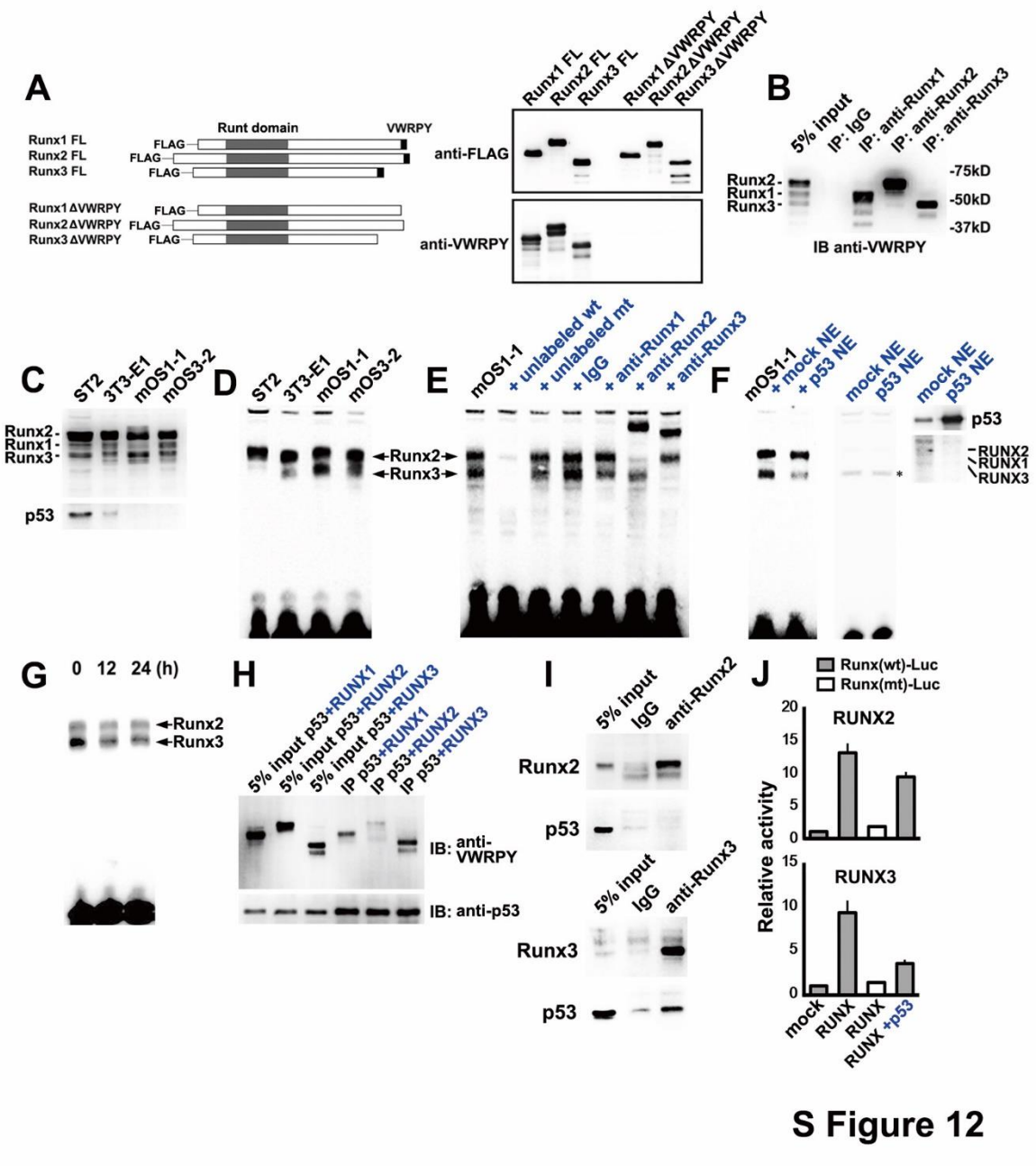
A
Runt domain
VWRPY
Runx1 FL
Runx2 FL
Runx3 FL
Runx1 ΔVWRPY
Runx2 ΔVWRPY
Runx3 ΔVWRPY
FLAG
anti-FLAG
anti-VWRPY
B
5% input
IP: IgG
IP: anti-Runx1
IP: anti-Runx2
IP: anti-Runx3
Runx2
Runx1
Runx3
-75kD
-50kD
-37kD
IB anti-VWRPY
C
ST2
3T3-E1
mOS1-1
mOS3-2
p53
D
E
mOS1-1
+ unlabeled wt
+ unlabeled mt
+ IgG
+ anti-Runx1
+ anti-Runx2
+ anti-Runx3
F
mOS1-1
+ mock NE
+ p53 NE
mock NE
p53 NE
p53
RUNX2
RUNX1
RUNX3
G
0 12 24 (h)
H
5% input p53+RUNX1
5% input p53+RUNX2
5% input p53+RUNX3
IP p53+RUNX1
IP p53+RUNX2
IP p53+RUNX3
IB: anti-VWRPY
IB: anti-p53
I
5% input
IgG
anti-Runx2
anti-Runx3
J
Runx(wt)-Luc
Runx(mt)-Luc
RUNX2
RUNX3
Relative activity
mock
RUNX
RUNX
RUNX +p53

S Figure 12

Supplementary Figure 12. p53 attenuates DNA binding and transactivation of Runx3.
(A) Pan-reactivity against Runx1–3 proteins of an anti-VWRPY mouse monoclonal antibody established for this study. Exogenously expressed FLAG-tagged RUNX/Runx1–3 (left) was detected specifically and evenly by the anti-VWRPY antibody similarly to the anti-FLAG antibody, as determined by western blotting (right). (B) Endogenous amounts and proportions of Runx1–3 in the nuclear extract (NE) of ST2 (a mouse BM-MSC line) cells, detected with the anti-VWRPY antibody (Input). Immunoprecipitates of the NE with specific antibodies against each Runx family member were also subjected to western blotting to identify each Runx in the NE. (C) Endogenous amounts of Runx1–3 and p53 proteins in NEs of ST2, 3T3-E1 (a mouse preosteoblastic cell line), mOS1-1, and mOS3-2 (clone 2 of mOS3 shown in Supplementary Fig. 2C). Runx1–3 were detected using the anti-VWRPY antibody. (D) EMSA using NEs shown in (C) and a labeled DNA probe with an intact mR1 sequence (wt). (E) EMSA using NE from mOS1-1 cells, a labeled wt probe, unlabeled wt or mutated mR1 (mt) probes, and normal IgG, anti-Runx1, anti-Runx2, or anti-Runx3 antibodies. The positions of probe-Runx2 and -Runx3 complexes are indicated. (F) Inhibition of Runx3–probe binding by p53. NE from mOS1-1 cells was mixed with NE of mock 293T cells or cells expressing exogenous p53, and then subjected to EMSA using a labeled wt probe (left). EMSA using only NE from mock 293T cells or cells expressing exogenous p53 and a labeled wt probe (center). Amounts of exogenous p53 and endogenous RUNX1–3 in NE of 293T cells added to the EMSA were determined by western blotting (right). The asterisk shows a non-specific protein–probe complex. (G) EMSA using NE of p53-induced mOS1-1 cl.1 (0, 12, and 24 h) (Supplementary Fig. 11A) and a labeled wt probe. (H) Interactions between p53 and RUNX proteins. Immunoprecipitates of whole-cell extracts of 293T cells expressing exogenous p53 and RUNX1, RUNX2, or RUNX3 with an anti-p53 antibody were subjected to western blotting. (I) Interactions between endogenous p53 and Runx3 proteins in NE of ST2 cells. Immunoprecipitates of NE of ST2 cells generated with anti-Runx2 or anti-Runx3 antibodies were subjected to western blotting. (J) Effect of p53 on transactivation of RUNX2 or RUNX3 in G292 cells (n=3).

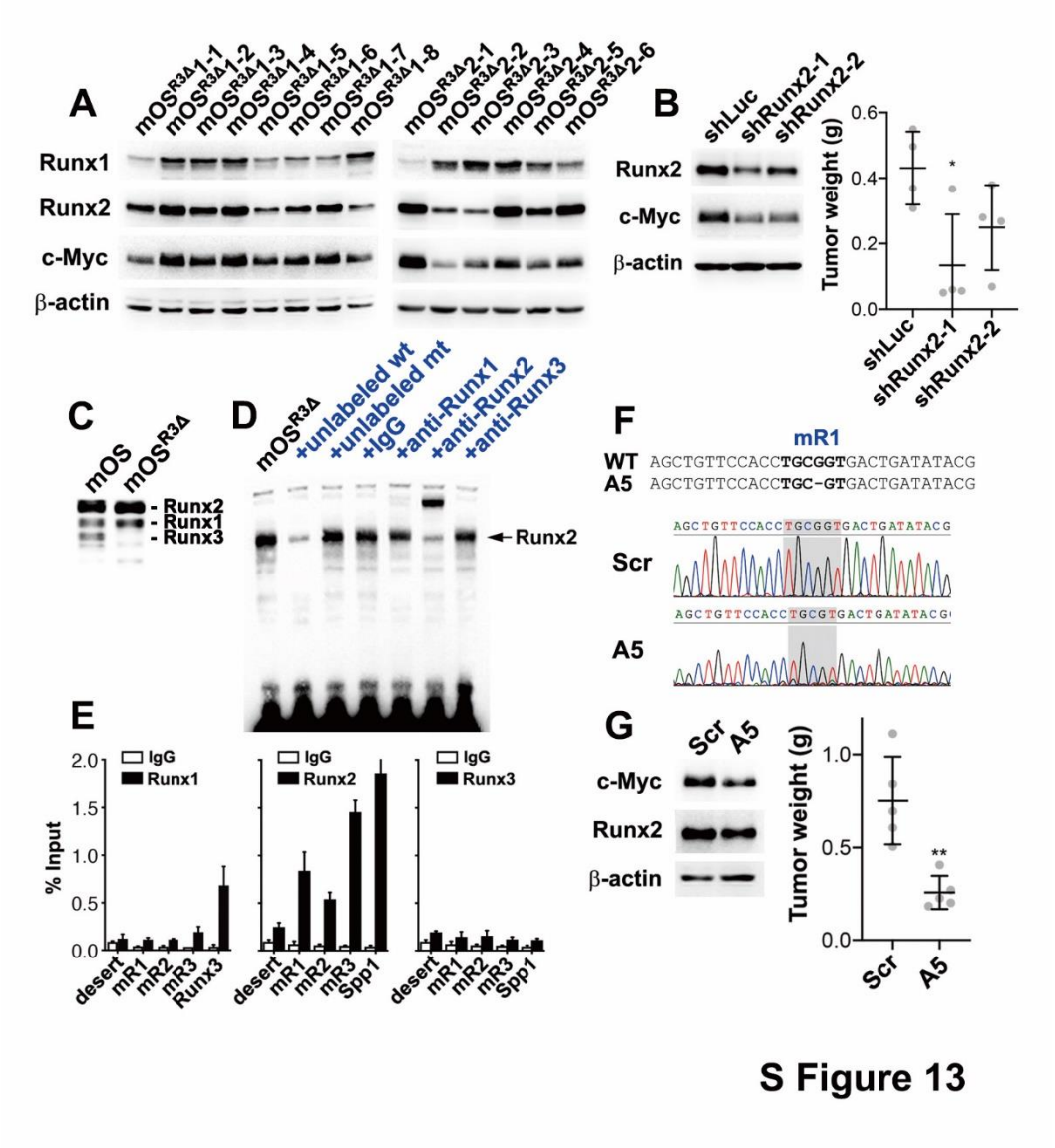

S Figure 13

Supplementary Figure 13. Oncogenic role of Runx2 in *Runx3*-deficient mOS cells.
(A) Levels of the indicated proteins in clones of *Runx3*-deficient mOS ($mOS^{R3\Delta}1$ and $mOS^{R3\Delta}2$) cells, which were isolated from OS developed in two individual *OS*; $Runx3^{fl/fl}$ mice, as determined by western blotting. (B) Effects of knockdown of Runx2 on the tumorigenicity of $mOS^{R3\Delta}2$-1 cells. Levels of the indicated proteins in the cells were determined by western blotting (left), and their tumorigenicity was evaluated by the allograft (right). (C) Endogenous levels of Runx1–3 in NE of $mOS^{R3\Delta}$1-3 cells, as determined by western blotting with anti-VWRPY antibody. (D) EMSA using NE from $mOS^{R3\Delta}$1–3 cells, labeled wt probe, unlabeled wt or mt probes, and normal IgG, anti-Runx1, anti-Runx2, or anti-Runx3 antibodies. Positions of probe–Runx2 complex is indicated. (E) Occupancy of Runx1–3 on each genomic element in $mOS^{R3\Delta}$1–3 cells. (F) Genome-edited $mOS^{R3\Delta}$1–3 cell line bearing a 1 bp homozygous deletion in mR1 (A5) and the control line (Scr). (G) Levels of the indicated proteins in Scr and A5 $mOS^{R3\Delta}$1-3 cells were determined by western blotting, and the tumorigenicity of each cell line is shown. $^{**}p < 0.01$; $^{*}p < 0.05$.

Supplementary Table 1. Common 47 TFs up- or down-regulated in human and mouse OS.

	Human OS RNA-seq					Mouse OS RNA-seq				
	Gene	avg. ex.	log2FC	p value	q value	Gene	avg. ex.	log2FC	p value	q value
1	*BHLHE40*	12.160	1.205	0.247	0.457	*Myc*	11.576	1.882	0.006	0.037
2	*JUNB*	12.110	1.518	0.113	0.276	*Fos*	11.397	1.103	0.141	0.388
3	*FOS*	11.765	2.508	0.248	0.458	*Bhlhe40*	11.196	1.290	0.013	0.070
4	*MYC*	11.698	1.950	0.095	0.245	*Etv1*	10.686	-1.891	0.000	0.000
5	*LITAF*	11.357	2.025	0.004	0.023	*Snai1*	10.232	1.069	0.148	0.399
6	*EBF3*	10.521	-1.762	0.023	0.091	*Runx3*	9.962	2.166	0.001	0.009
7	*RUNX3*	9.902	4.961	0.000	0.000	*Bhlhe41*	9.806	1.070	0.139	0.385
8	*ETV1*	9.780	-1.142	0.166	0.356	*Litaf*	9.431	1.414	0.009	0.055
9	*IRF7*	9.709	1.135	0.300	0.515	*Junb*	9.416	1.370	0.015	0.080
10	*MZF1*	9.707	-1.324	0.006	0.035	*Heyl*	9.261	1.549	0.051	0.199
11	*BHLHE41*	9.438	2.261	0.088	0.233	*Irf7*	8.879	2.574	0.000	0.004
12	*HOXC10*	9.379	2.134	0.002	0.014	*Atf3*	8.810	1.647	0.091	0.291
13	*PITX1*	9.379	2.512	0.033	0.118	*Prdm1*	8.582	1.096	0.185	0.454
14	*FOSL1*	9.220	1.267	0.440	0.649	*Ebf2*	8.279	-2.961	0.000	0.000
15	*PRDM1*	8.655	2.610	0.004	0.024	*Fosl1*	8.138	3.320	0.006	0.039
16	*HOXC4*	8.532	1.313	0.127	0.297	*Nr6a1*	7.862	1.463	0.021	0.102
17	*RFX8*	8.465	-1.139	0.106	0.264	*Irf8*	7.852	2.690	0.000	0.001
18	*HOXA5*	8.191	1.116	0.182	0.377	*Foxd1*	7.706	-5.129	0.000	0.000
19	*HOXA7*	8.159	2.510	0.007	0.036	*Hoxa3*	7.484	2.516	0.002	0.016
20	*SNAI1*	8.156	4.190	0.002	0.013	*Hsf4*	7.033	1.898	0.029	0.132
21	*ATF3*	8.096	2.213	0.076	0.210	*Aknad1*	6.825	1.116	0.294	0.592
22	*HOXB3*	7.892	3.696	0.000	0.002	*Rorc*	6.734	-2.965	0.000	0.004
23	*HOXB2*	7.885	4.429	0.000	0.000	*Hoxb2*	6.672	2.544	0.022	0.106
24	*HSF4*	7.830	1.508	0.257	0.468	*Pou2f2*	6.650	1.120	0.143	0.391
25	*HOXA3*	7.783	1.324	0.246	0.455	*Foxf1*	5.932	1.763	0.114	0.340
26	*EBF2*	7.770	-1.064	0.109	0.270	*Hoxc10*	5.895	5.879	0.000	0.002
27	*POU2F2*	7.627	4.666	0.009	0.047	*Rorb*	5.890	-2.016	0.038	0.161
28	*LHX4*	7.149	-1.283	0.085	0.229	*Hoxa5*	5.684	3.642	0.000	0.004
29	*HEYL*	7.148	8.564	0.000	0.000	*Hoxb3*	5.683	2.221	0.024	0.113
30	*SNAI3*	7.126	-1.995	0.000	0.004	*Hoxc4*	5.316	4.243	0.000	0.001
31	*FOXD1*	7.044	-4.595	0.000	0.000	*Rfx8*	5.154	-1.091	0.153	0.407
32	*HOXC11*	7.038	1.139	0.356	0.572	*Hoxa7*	5.122	4.386	0.000	0.003
33	*NR6A1*	6.999	1.537	0.079	0.218	*Mzf1*	5.037	-1.145	0.112	0.336
34	*RORB*	6.661	-1.008	0.314	0.529	*Batf2*	4.894	1.634	0.050	0.196
35	*HOXB6*	6.608	4.119	0.000	0.001	*Foxp3*	4.864	1.409	0.085	0.280
36	*HOXB7*	6.540	6.186	0.000	0.000	*Hoxb4*	4.829	3.468	0.001	0.007
37	*HOXB4*	6.414	4.079	0.000	0.005	*Ebf3*	4.374	-2.985	0.000	0.001
38	*RORC*	5.727	-1.264	0.175	0.368	*Pitx1*	4.230	1.268	0.624	0.856
39	*DLX4*	5.560	10.004	0.000	0.002	*Hoxb6*	4.196	3.463	0.005	0.034
40	*BATF2*	5.358	4.214	0.024	0.095	*Dlx4*	4.155	1.058	0.345	0.645
41	*AKNAD1*	5.239	1.822	0.143	0.322	*Hoxc11*	4.117	5.434	0.010	0.057
42	*IRF8*	5.178	6.577	0.000	0.000	*Hoxb7*	3.736	4.360	0.001	0.010
43	*SIX6*	4.414	-1.825	0.140	0.318	*Hoxb5*	3.318	4.126	0.001	0.009
44	*FOXF1*	4.061	5.851	0.056	0.171	*Lhx4*	3.162	-3.007	0.000	0.002
45	*HOXB5*	3.941	6.620	0.000	0.001	*Pou1f1*	2.437	-2.329	0.008	0.048
46	*FOXP3*	3.886	2.557	0.087	0.232	*Snai3*	2.402	-2.155	0.027	0.123
47	*POU1F1*	2.457	1.085	0.314	0.530	*Six6*	0.670	1.316	0.333	0.633

Supplementary Table 2. Runx3 target genes (95 genes) in the *p53*-deficient context.

		ChIP merged peak				Array
	Gene	Score	Chr	Start	End	log2FC
1	*Myc*	314.2	chr15	62328449	62328642	0.61
2	*Gjb4*	149.8	chr4	127352680	127352864	1.68
3	*Ywhae*	113.1	chr11	75737056	75737217	0.39
4	*Trmt112*	81.2	chr19	6909618	6909797	0.47
5	*Got1*	78.0	chr19	43512028	43512212	0.44
6	*Eef2*	76.8	chr10	81176443	81176577	0.39
7	*Tm4sf1*	74.7	chr3	57093681	57093865	0.53
8	*Usp36*	71.0	chr11	118290235	118290448	0.81
9	*Ube2f*	70.8	chr1	91250118	91250395	0.39
10	*Eef1a1*	64.2	chr9	78481855	78481973	0.30
11	*Magohb*	61.8	chr6	131298615	131298766	0.55
12	*Shoc2*	59.5	chr19	53944041	53944246	0.52
13	*Ywhaz*	58.8	chr15	36742686	36742978	0.63
14	*Zdhhc18*	58.3	chr4	133631581	133631805	0.58
15	*Itpr3*	56.7	chr17	27056272	27056499	0.65
16	*Cct6a*	56.6	chr5	129787239	129787449	0.68
17	*Sertad2*	54.6	chr11	20469468	20469705	0.60
18	*Rps28*	54.4	chr17	33824438	33824659	0.38
19	*Polh*	50.3	chr17	46202499	46202736	0.66
20	*Ddx23*	46.1	chr15	98662903	98663030	0.39
21	*Eif2s3x*	46.0	chrX	94177746	94178020	0.79
22	*Shb*	44.1	chr4	45473190	45473360	0.61
23	*Ncl*	44.1	chr1	86359377	86359603	0.56
24	*Fermt2*	40.8	chr14	45530058	45530239	0.58
25	*Osbpl3*	40.0	chr6	50355439	50355591	0.61
26	*Ttll7*	37.7	chr3	147298120	147298317	0.53
27	*Gdnf*	36.7	chr15	7931711	7931903	1.34
28	*Sla*	33.9	chr15	66844080	66844246	1.42
29	*Gtf2a2*	33.9	chr9	70012453	70012631	0.42
30	*Fam49b*	33.8	chr15	64006172	64006373	0.65
31	*Kbtbd11*	33.8	chr8	14992834	14992999	2.15
32	*Atg5*	33.7	chr10	44268231	44268490	0.32
33	*Rpl5*	33.5	chr5	107938626	107938801	0.34
34	*Cacybp*	33.2	chr1	160234081	160234286	0.70
35	*Abcf1*	33.0	chr17	35969721	35969911	0.43
36	*Aebp2*	32.8	chr6	140780930	140781093	0.56
37	*Lsm5*	32.6	chr6	56655465	56655742	0.32
38	*Coro1c*	32.2	chr5	113930979	113931142	0.66
39	*Klhl32*	31.5	chr4	24788599	24788788	0.82
40	*Tmem161b*	31.3	chr13	84371156	84371323	0.41
41	*AI314180*	31.3	chr4	58867381	58867490	0.31
42	*Rrn3*	31.0	chr16	13780629	13780822	0.48
43	*Senp2*	30.9	chr16	22076575	22076805	0.43
44	*Zc3h18*	30.1	chr8	122376531	122376696	0.39
45	*Nras*	30.1	chr3	103058244	103058433	0.33
46	*Pitpnb*	30.1	chr5	111228472	111228670	0.47
47	*Loxl4*	29.3	chr19	42631632	42631849	1.89
48	*Ptk2b*	29.2	chr14	66221116	66221322	0.92

Supplementary Table 2. (continued)

		ChIP merged peak				Array
	Gene	Score	Chr	Start	End	log2FC
49	*Msn*	28.6	chrX	96086344	96086514	0.80
50	*Ncor2*	28.6	chr5	125245828	125246041	0.22
51	*Hnrnpa3*	26.6	chr2	75622336	75622482	0.43
52	*Zfp428*	26.5	chr7	24507247	24507519	0.43
53	*Abce1*	26.5	chr8	79679038	79679228	0.65
54	*Hnrnpf*	25.1	chr6	117895552	117895751	0.29
55	*Zfp706*	24.2	chr15	36960454	36960643	0.51
56	*Tmem131*	24.1	chr1	37030761	37030932	0.37
57	*Rpl31*	22.6	chr1	39349167	39349273	0.41
58	*Fdx1l*	22.1	chr9	21073490	21073676	0.43
59	*Btg3*	22.0	chr16	78451490	78451682	0.32
60	*Tbc1d1*	20.9	chr5	64298395	64298615	0.32
61	*Atp13a3*	20.8	chr16	30439549	30439775	0.22
62	*Zfp35*	20.6	chr18	23989537	23989641	0.41
63	*Alkbh8*	20.6	chr9	3335400	3335590	0.39
64	*Thada*	20.5	chr17	84466146	84466388	0.35
65	*Snrpc*	20.1	chr17	27839985	27840107	0.46
66	*Hs6st1*	18.0	chr1	35935342	35935506	0.44
67	*Gls*	17.4	chr1	52254535	52254792	0.79
68	*Impad1*	17.3	chr4	4987635	4987754	0.39
69	*Klc2*	17.2	chr19	5178643	5178837	0.77
70	*Ivns1abp*	16.8	chr1	151289579	151289733	0.45
71	*Mif*	16.7	chr10	75872965	75873100	0.81
72	*Fam72a*	16.0	chr1	131552046	131552165	0.47
73	*Pvr*	16.0	chr7	19911334	19911544	0.92
74	*Hnrnpk*	15.8	chr13	58443938	58444049	0.27
75	*Zmym1*	15.6	chr4	127061069	127061224	0.43
76	*Rtkn2*	15.3	chr10	67984319	67984548	0.81
77	*Cdh18*	15.2	chr15	23682197	23682389	0.37
78	*March6*	15.1	chr15	31542691	31542893	0.14
79	*Taf5*	15.0	chr19	47067584	47067804	0.59
80	*Nkrf*	14.0	chrX	36903374	36903542	0.76
81	*Tspan2*	13.9	chr3	102649230	102649367	1.34
82	*Rpl34*	13.8	chr3	130827979	130828159	0.39
83	*Fyn*	12.6	chr10	39335950	39336144	1.10
84	*Siglech*	12.0	chr7	55539955	55540157	0.45
85	*Rsl24d1*	11.2	chr9	73165753	73165906	0.43
86	*Pinx1*	10.3	chr14	63860814	63861030	0.90
87	*Mospd4*	10.3	chr18	46405082	46405294	1.33
88	*Ecsit*	9.0	chr9	22090113	22090271	0.60
89	*Panx1*	8.9	chr9	15045442	15045689	0.56
90	*Anp32b*	8.8	chr4	46433734	46433933	0.22
91	*Rock2*	8.5	chr12	16886599	16886811	0.37
92	*Pcgf6*	7.1	chr19	47050319	47050498	0.62
93	*Ets1*	6.8	chr9	32629549	32629683	0.49
94	*Ttc14*	6.7	chr3	33498657	33498913	0.93
95	*Ube2q2*	5.7	chr9	55126410	55126562	0.85

Supplementary Table 3. ChIP-qPCR primers.

Primer Name	Sequences
Mouse gene desert	5’-ACCAAGCACAGAAAAGGTTCAAAC-3’ and 5’-TCCAGATGCTGAGAGAAAAACAAC-3’
mR1	5’-GCCTTAGAGAGACGCCTGGC-3’ and 5’-CCGCAGGTGGAACAGCTGC-3’
mR2	5’-GTGGCAGTGAGTTGCTGAGC-3’ and 5’-GAAAGGGGGAAGGACGAACG-3’
mR3	5’-CCCTCGTTGGCTTCGCAACG-3’ and 5’-ACCCGGGTTGTGGCTCTCG-3’
Spp1 promoter	5’-AATGACATCGTTCATCAGTAATGC-3’ and 5’-CATGAGGTTTTTGCCACTACC-3’
Gapdh promoter	5’-GGACTGCCTGGTGTCCTTCG-3’ and 5’-TCACCCGTTCACACCGACC-3’
Runx3 P1 promoter	5’-ACACTGGGAAGGTCTGGTCC-3’ and 5’-AGGAACCAACCAGCTCCTCG-3’
Myc P1 promoter	5’-CCCTTTATATTCCGGGGGTCTGC-3’ and 5’-CGAAGCCCTGCCCTTCAGG-3’
Myc P2 promoter	5’-TCGCAGTATAAAAGAAGCTTTTCGG-3’ and 5’-CACACACGGCTCTTCCAACC-3’
Myc P3 promoter	5’-CAGACAGCCACGACGATGC-3’ and 5’-CTTCCTCGTCGCAGATGAAATAGG-3’
Myc -0.1k	5’-CCTCCCGAGTTCCCAAAGC-3’ and 5’-CGGGGATTAGCCAGAGAATCTC-3’
Myc +0.3k	5’-GCTTTGCCTCCGAGCCTGC-3’ and 5’-GCAATGGGCAAAGTTTCCCAGC-3’
Myc +0.5k	5’-GTCTATTTGGGGACAGTGTTCTCTG-3’ and 5’-GGGTTTCCAACGCCCAAAGG-3’
Myc Exon2	5’-GTACCTCGTCCGATTCCACG-3’ and 5’-CAGCACTAGGGGCTCAGG-3’
Myc Exon3	5’-TCTCGTGAGAGTAAGGAGAACG-3’ and 5’-CTGAAGCTTACAGTCCCAAAGC-3’
Human gene desert	5’-TGAGCATTCCAGTGATTTATTG-3’ and 5’-AAGCAGGTAAAGGTCCATATTTC-3’
MR1	5’-CCTGCGATGATTTATACTCACAGG-3’ and 5’-AAACCCTCTCCCTTTCTCTGC-3’
MR2	5’-GCACGGAAGTAATACTCCTCTCC-3’ and 5’-GACGTTTAATTCCTTTCCAGGTCC-3’
MR3	5’-GGGTGATGTTCATTAGCAGTGG-3’ and 5’-GAAGAAAGAGGAGTTACTGGAGG-3’
SPP1 promoter	5’-TTTAACTGTAGATTGTGTGTGTGC-3’ and 5’-ATTGTGTCATGAGGTTTTCTGC-3’
RUNX3 P1 promoter	5’-CACTGGGAAGGCCTGGTCC-3’ and 5’-GCACCAGGAGCCAACCAGC-3’

Supplementary Table 4. sgRNAs used for epigenome editing

sgRNA	sequences
Scrambled	5’-TGGTTTACATGTCGACTAAC-3’
Myc -740k	5’-TCCATATAAGTGACTGAATG-3’
Myc -450k	5’-GCACCTAGGCATCCCACTTG-3’
Myc mR3	5’-TCGTTGGCTTCGCAACGCTG-3’
Myc mR2	5’-ACCGCAGATGAGGTCTATGC-3’
Myc mR1	5’-CTGCGTATATCAGTCACCGC-3’
Myc TSS	5’-CGCTCCGGGGCGACCTAAGA-3’
Myc +300k	5’-CCTTAAACTCAACCCTCCAG-3’
Myc +340k	5’-CAGAACCAATAAGAGCGGTG-3’
Myc +710k	5’-ATAAGTTCAGAACATTCTGT-3’
Myc +1.1M	5’-GTGCCAGCAGATTCACCTCT-3’
Myc N-Me	5’-GCTGATGATTTCAGTCAATT-3’
Myc BDME-E3	5’-ACACAGTGTGGTTCCTTTTC-3’

References

1 Jiang Q, Qin X, Kawane T, Komori H, Matsuo Y, Taniuchi I *et al.* Cbfb2 Isoform Dominates More Potent Cbfb1 and Is Required for Skeletal Development. *J Bone Miner Res* 2016; **31**: 1391–1404.

2 Ito K, Inoue K, Bae S-C, Ito Y. Runx3 expression in gastrointestinal tract epithelium: resolving the controversy. *Oncogene* 2009; **28**: 1379–1384.

3 Bray NL, Pimentel H, Melsted P, Pachter L. Near-optimal probabilistic RNA-seq quantification. *Nat Biotechnol* 2016; **34**: 525–527.

4 Sun J, Nishiyama T, Shimizu K, Kadota K. TCC: an R package for comparing tag count data with robust normalization strategies. *Bmc Bioinformatics* 2013; **14**: 219.

5 Mizoguchi T, Pinho S, Ahmed J, Kunisaki Y, Hanoun M, Mendelson A *et al.* Osterix marks distinct waves of primitive and definitive stromal progenitors during bone marrow development. *Dev Cell* 2014; **29**: 340–9.

6 Mohseny AB, Machado I, Cai Y, Schaefer K-L, Serra M, Hogendoorn PCW *et al.* Functional characterization of osteosarcoma cell lines provides representative models to study the human disease. *Lab Invest* 2011; **91**: 1195–1205.

7 Lauvrak SU, Munthe E, Kresse SH, Stratford EW, Namløs HM, Meza-Zepeda LA *et al.* Functional characterisation of osteosarcoma cell lines and identification of mRNAs and miRNAs associated with aggressive cancer phenotypes. *Brit J Cancer* 2013; **109**: 2228–2236.

8 Motoyama T, Hotta T, Watanabe H, Kumanishi T, Ichikawa T, Sekiguchi M. Differential production of interleukin 6 in human osteosarcoma cells and the possible effects on neoplastic bone metabolism. *Virchows Archiv B* 1993; **63**: 277–281.

9 Spender LC, Whiteman HJ, Karstegl CE, Farrell PJ. Transcriptional cross-regulation of RUNX1 by RUNX3 in human B cells. *Oncogene* 2005; **24**: 1873–1881.

10 Whittle MC, Izeradjene K, Rani PG, Feng L, Carlson MA, DelGiorno KE *et al.* RUNX3 Controls a Metastatic Switch in Pancreatic Ductal Adenocarcinoma. *Cell* 2015; **161**: 1345–60.